seven repeats of CGG, while the minor one contained eight (Table 1). As far as we examined, we did not find repeat numbers other than seven or eight. The repeat is conserved among vertebrates, since chicken, mouse, and rat *PTCH* contain four or five repeats of CGG (Fig. 1C). However, the repeat has not been found in Xenopus *PTCH*, indicating it is not conserved in amphibians.

Abnormal expansion of the CGG triplet repeat in the 5'-UTR of the *fragile X mental retardation-1* (*FMR1*) gene is responsible for fragile X syndrome, in which the repeat is abnormally hypermethylated, resulting in the silence of the *FMR1* (reviewed by Jin et al. 2000). Since CGG repeat in *PTCH* is immediately upstream of the first in-frame methionine codon, the repeat number may influence the efficiency of translation as well as of transcription. To address this issue, various lengths of $(CGG)_nCAAC$ were subcloned into the luciferase plasmid pGV-P2 between the SV40 promoter and the coding sequence for luciferase (Fig. 2A), and luciferase assays were performed. Luciferase activities gradually increased with the number of CGG repeats, at least within the range we examined. The highest level of luciferase activity was obtained when cells were transfected with the plasmid pGV-$(CGG)_{19}CG(CGG)_6$, which was generated by chance during PCR reaction (Fig. 2B). These results suggest that individuals with $(CGG)_8/(CGG)_8$ have higher levels of PTCH protein expression than those with $(CGG)_7/(CGG)_7$. This is contradictory to the case of *FMR1*. However, it should be noted that in fragile X syndrome, the repeat is massively expanded over 230, and the repeat is located more than 50 bp upstream of the first methionine codon.

To address the question of whether the difference in luciferase activity is transcriptional or translational, the levels of luciferase RNA expression were quantified by a real-time RT-PCR. As shown in Fig. 2C, in contrast to the activities of luciferase, no significant difference in luciferase transcription was observed. Moreover, unexpectedly, the cells transfected with the plasmid pGV-$(CGG)_{19}CG(CGG)_6$ expressed significantly lower levels of luciferase RNA. Therefore, the increase in luciferase activities with the expansion of the CGG repeat is due to the increased efficiency of translation.

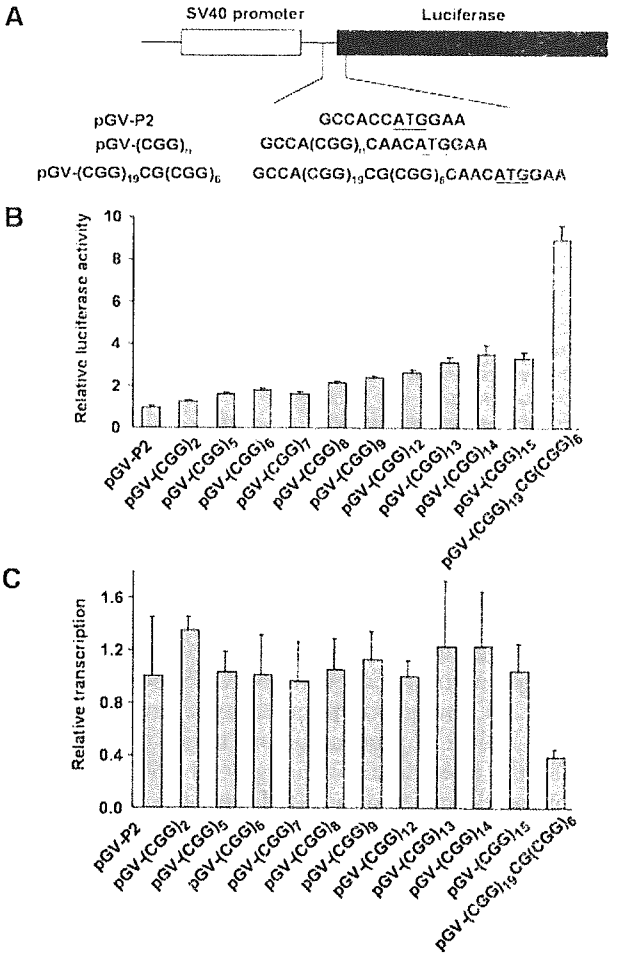

Fig. 2 **A** Schematic depiction of reporter gene constructs used for a luciferase assay. Nucleotide sequences inserted between SV40 promoter and the luciferase gene are indicated at the *bottom*. The first methionine codon of the luciferase gene is *underlined*. **B** The effect of the repeat length on luciferase activities; 293 cells transfected with plasmids indicated at the *bottom* were harvested 24 h after the transfection and subjected to a luciferase assay. **C** The effect of the repeat length on luciferase transcriptions. Total RNA was extracted from 293 cells transfected with plasmids indicated at the *bottom* and subjected to a real-time RT-PCR. Luciferase transcriptions were normalized by those of *GAPDH*

Table 1 Genotype data of a $(CGG)_n$ on the *PTCH* gene

	Controls	NBCCS
Major allele (repeat number: 7) [%]	88 [86.3]	25 [89.3]
Minor allele (repeat number: 8) [%]	14 [13.7]	3 [10.7]
Total	102 [100.00]	28 [100.00]
Major homozygous [%]	39 [76.5]	12 [85.7]
Heterozygous [%]	10 [19.6]	1 [7.1]
Minor homozygous [%]	2 [3.9]	1 [7.1]
Total	51 [100.0]	14 [100.0]
χ^2 [*P*]		
Genotype frequency (2×3 table)	1.38 [0.50]	
Allele frequency (major versus minor)	0.18 [0.68]	
Major homozygous versus others	0.56 [0.46]	
Minor homozygous versus others	0.26 [0.61]	
Odds ratio [95% CI]		
Major homozygous versus others	1.85 [0.36–9.43]	
Minor homozygous versus others	1.88 [0.16–22.44]	
Major allele versus minor allele	0.75 [0.20–2.83]	

Table 2 CGG/CCG-containing genes. *UTR* untranslated region

	$(CGG)_n$	$(CCG)_n$	Total
CDS	39	29	68
5' UTR	95[a]	51[a]	146
Total	134	80	214

Genes with a repeat of seven or more CGG/CCG were downloaded from NCBI nucleotide databases:
[a]The number of CGG-containing genes are significantly higher than CCG-containing genes (χ^2 test, $P = 0.00027$)

Table 3 $(CGG)_n/(CCG)_n$-containing genes in which the triplet repeat is located immediately upstream of the first in-frame methionine codon

Accession no.[a]	Gene[b]	Nucleotides between $(CGG)_n/(CCG)_n$ and ATG	CGG or CCG	n
BC029158	Clone MGC:34313 IMAGE:5198758	CCCCCGGGGC	CCG	10
NM_025075	Hypothetical protein FLJ23445	CGCACGCC	CCG	8
BC015930	Clone MGC:8881 IMAGE:3920963	CGGGGGCC	CCG	8
NM_013396	Ubiquitin specific protease 25 (USP25)	CGGGGGCC	CCG	8
NM_013272	Solute carrier family 21 (organic anion transporter), member 11 (SLC21A11)	GGGAAGG	CGG	8
NM_005360	Transcription factor C-MAF (c-maf)	CAGGAGA	CGG	7
NM_004699	DNA segment on chromosome X (unique) 9928 expressed sequence (DXS9928E) (XAP-5)	CTGCC	CCG	9
NM_000264	PTCH	CAAC	CGG	7
NM_145296	TSLC1-like 2 (TSLL2)	CACC	CGG	7
NM_002958	RYK receptor-like tyrosine kinase (RYK)	CCC	CGG	7
NM_017811	Ubiquitin-conjugating enzyme E2R 2 (UBE2R2)	CG	CCG	7
NM_173054	Reelin (RELN)	C	CGG	8–10[c]

[a]One representative accession number for one gene
[b]Genes that have less than ten nucleotides between triplet repeat and the first methionine
[c]Repeat number varies depending on deposited sequences

The distributions of genotypes that we observed in NBCCS patients and controls did not differ from the expected frequencies under the assumption of Hardy-Weinberg equilibrium (data not shown), nor were significant associations with NBCCS observed (Table 1). Thus far, no genotype-phenotype correlation between the position of mutations and major clinical features of NBCCS is evident (Wicking et al. 1997b). Since developmental defects associated with the disorder are most likely due to haploinsufficiency, and the repeat length potentially alter the expression levels of PTCH, the repeat number may have an effect on the severity of the disease. It would also be interesting to examine the association of the repeat number with sporadic or non-inherited basal cell carcinoma or medulloblastoma, since PTCH acts as a tumor suppressor in these tumors (reviewed by Hunter 1997).

In order to find other genes with CGG repeats, we next performed a genome-wide screening of CGG/CCG-containing genes from NCBI nucleotide databases. A total of 214 genes having seven or more of the repeat number were downloaded. A complete list of the CGG/CCG-containing genes can be obtained from our Web site, http://genetics.nch.go.jp/supplements.htm. Of those 214 genes, 146 (68.2%) contained the repeat in the 5'-UTR (Table 2). Interestingly, significantly more genes have CGG repeats than CCG repeats (65.1% versus 34.9%, $P=0.00027$). More significantly, none of the downloaded genes contained repeats in the 3'-UTR. The genes containing CGG/CCG repeats in close proximity to their first methionine codons are listed in Table 3. Only five genes including *PTCH* have intervening sequences of up to 4 bp between $(CGG)_n/(CCG)_n$ and ATG. In this regard, *PTCH* is quite unique in terms of the location of the repeat. Considering our results, polymorphisms of the repeat number that might exist in these genes potentially affect their expression levels.

Acknowledgements We would like to thank the patients and family members as well as the clinicians who contributed to this study. We gratefully acknowledge assistance from Mami U, Kaori Inoue, and Kayoko Saito. This study was supported in part by grants for Brain Research, Pediatric Research, Cancer Research, and Genome Research from the Ministry of Health and Welfare, and a Grant-in-Aid for Scientific Research and the Budget for Nuclear Research from the Ministry of Education, Culture, Sports, Science, and Technology.

References

Fujii K, Miyashita T, Takanashi J, Sugita K, Kohno Y, Nishie H, Yasumoto S, Furue M, Yamada M (1999) γ-irradiation deregulates cell cycle control and apoptosis in nevoid basal cell carcinoma syndrome-derived cells. Jpn J Cancer Res 90:1351–1357

Fujii K, Kohno Y, Sugita K, Nakamura M, Moroi Y, Urabe K, Furue M, Yamada M, Miyashita T (2003a). Mutations in the human homologue of *Drosophila patched* in Japanese nevoid basal cell carcinoma syndrome patients. Hum Mutat 21:451–452

Fujii K, Miyashita T, Omata T, Kobayashi K, Takanashi J, Kouchi K, Yamada M, Kohno Y (2003b) Gorlin syndrome with ulcerative colitis in a Japanese girl. Am J Med Genet 121:65–68

Gorlin RJ (1987) Nevoid basal-cell carcinoma syndrome. Medicine 66:98–113

Hahn H, Wicking C, Zaphiropoulous PG, Gailani MR, Shanley S, Chidambaram A, Vorechovsky I, Holmberg E, Unden AB, Gillies S, Negus K, Smyth I, Pressman C, Leffell DJ, Gerrard B, Goldstein AM, Dean M, Toftgard R, Chenevix-Trench G, Wainwright B, Bale AE (1996) Mutations of the human homolog of Drosophila *patched* in the nevoid basal cell carcinoma syndrome. Cell 85:841–851

Hunter T (1997) Oncoprotein networks. Cell 88, 333–346

Imai Y, Matsushima Y, Sugimura T, Terada M (1991) A simple and rapid method for generating a deletion by PCR. Nucleic Acids Res 19:2785

Jin P, Warren ST (2000) Understanding the molecular basis of fragile X syndrome. Hum Mol Genet 9:901–908

Johnson RL, Rothman AL, Xie J, Goodrich LV, Bare JW, Bonifas JM, Quinn AG, Myers RM, Cox DR, Epstein EH, Jr, Scott MP (1996). Human homolog of *patched*, a candidate gene for the basal cell nevus syndrome. Science 272:1668–1671

Kimonis VE, Goldstein AM, Pastakia B, Yang ML, Kase R, DiGiovanna JJ, Bale AE, Bale SJ (1997) Clinical manifestations in 105 persons with nevoid basal cell carcinoma syndrome. Am J Med Genet 69:299–308

Shikama Y, U M, Miyashita T, Yamada M (2001) Comprehensive studies on subcellular localizations and cell death-Inducing activities of eight GFP-tagged apoptosis-related caspases. Exp Cell Res 264:315–325

Wicking C, Gillies S, Smyth I, Shanley S, Fowles L, Ratcliffe J, Wainwright B, Chenevix-Trench G (1997a) De novo mutations of the *patched* gene in nevoid basal cell carcinoma syndrome help to define the clinical phenotype. Am J Med Genet 73:304–307

Wicking C, Shanley S, Smyth I, Gillies S, Negus K, Graham S, Suthers G, Haites N, Edwards M, Wainwright B, Chenevix-Trench G (1997b). Most germ-line mutations in the nevoid basal cell carcinoma syndrome lead to a premature termination of the PATCHED protein, and no genotype-phenotype correlations are evident. Am J Hum Genet 60:21–26

Leukemia (2004) 18, 1850–1856

www.nature.com/leu

Identification of novel direct transcriptional targets of glucocorticoid receptor

M U[1], L Shen[1,2], T Oshida[3], J Miyauchi[4], M Yamada[1] and T Miyashita[1]

[1]*Department of Genetics, National Research Institute for Child Health and Development, Tokyo, Japan;* [2]*Department of Clinical Laboratory, Shanghai Children's Medical Center, Shanghai, China;* [3]*Discovery and Pharmacology Research Laboratories, Tanabe Seiyaku Co., Ltd, Saitama, Japan; and* [4]*Department of Clinical Laboratory, Tokyo Dental College Ichikawa General Hospital, Chiba, Japan*

Transcription of the genes *Granzyme A* (*GZMA*), *FK506 binding protein 51* (*FKBP5*), and *Down syndrome critical region gene 1* (*DSCR1*) is upregulated in leukemic cells upon treatment with glucocorticoids (GCs). Several lines of evidence suggest that these genes are implicated in GC-induced apoptosis upstream of the Bcl-2 family of proteins. These genes were upregulated by GC even in the presence of an inhibitor of protein synthesis, cycloheximide, indicating that they are direct target genes of glucocorticoid receptors. *DSCR1* is reported to have four isoforms, each of which has a distinct first exon, E1–E4. Among these isoforms, the one with E1 was selectively upregulated by GC. *GZMA* and *FKBP5* have a cluster of putative glucocorticoid response elements (GREs) in introns 1 and 2, respectively, that was identified to be responsible for the response to GC. They were composed of one complete (A/T)G(A/T)(A/T)C(A/T) sequence surrounded by two incomplete (A/T)G(A/T)(A/T)C(A/T) sequences separated by one to four nucleotides. *DSCR1*, however, did not have a functional GRE upstream or downstream of exon 1. These studies may lead to improved therapeutic uses of GCs in leukemia and lymphoma based upon the expression of these GC target genes.
Leukemia (2004) **18,** 1850–1856. doi:10.1038/sj.leu.2403516
Published online 23 September 2004
Keywords: ALL; glucocorticoid; granzyme A; FKBP51; DSCR1

Introduction

Glucocorticoids (GCs) are known to be potent immunosuppressive, antiallergic, and anti-inflammatory drugs. They exert their effects on target cells by binding to an intracellular glucocorticoid receptor (GR). The ability of GCs to induce apoptosis and cell cycle arrest in lymphoid cells has resulted in their widespread use as chemotherapeutic agents for various leukemias, lymphomas, and multiple myelomas, although the precise mechanism of their actions is yet to be elucidated.[1,2] Glucocorticoid receptor (GR) is a member of the nuclear hormone receptor superfamily localized in the cytoplasm. Inactive GR is bound to a large protein complex that includes heat shock protein 90 (Hsp90). When GC binds to GR, Hsp90 dissociates and the GC/GR complex translocates to the nucleus where it binds to specific palindromic sequences, termed glucocorticoid response elements (GREs), resulting in the transcriptional upregulation of various genes.[3]

We previously investigated transcriptional changes during GC-induced apoptosis in GC-sensitive human pre-B leukemia 697 cells harboring the t(1;19) chromosomal translocation[4] using oligonucleotide microarrays.[5] Among 93 genes induced by a synthetic GC, dexamethasone (DEX), were *Granzyme A* (*GZMA*), and two other genes encoding calcineurin inhibitors, *FK506 binding protein 51* (*FKBP5*) and *Down syndrome critical region gene 1* (*DSCR1*). Granzymes are serine proteases and are packaged in cytotoxic granules of CTL and NK cells, together with the pore-forming protein perforin. The concerted action of these molecules induces apoptosis of target cells, such as infected cells or transformed tumor cells.[6,7] *DSCR1*, a gene located on chromosome 21, is highly expressed in fetal brain and is suggested to have a role in brain development. The product of *DSCR1* interacts with the catalytic A subunit of calcineurin and inhibits its phosphatase activity, and thus is also called modulatory calcineurin-interacting protein 1 (MCIP1).[8] *FKBP5* encodes FK506 binding protein of 51 kDa, which is known as an immunophillin, and also regulates the inhibition of calcineurin.[9,10] These three genes are suggested to mediate GC-induced apoptosis in lymphoid cells by the following findings. First, the granzyme inhibitor 3,4-dichloroisocoumarin has been reported to inhibit DEX-induced apoptosis of 697 cells.[11] Second, the activation of calcineurin protects T cells from GC-induced apoptosis.[12,13] Moreover, using a variety of pre-B leukemic cells, the expression of the latter two genes evoked by GC and the induction of apoptosis were found to be closely correlated.[5] However, the induction of these genes does not necessarily mean that they are direct transcriptional targets, because they may be regulated via a secondary effect induced by the primary targets of GC. In addition, GR regulates transcription by binding to and inhibiting or enhancing the function of other transcription factors such as AP-1, NF-κB, and the STAT family of transcription factors, which can change the transcriptional profile.[14,15] Therefore, we investigated the genomic organization of these genes and whether they are direct target genes of GR.

Materials and methods

Cells and reagents

Pre-B human leukemia 697 cells were routinely grown in RPMI 1640 medium supplemented with 10% heat-inactivated fetal calf serum, 50 U/ml of penicillin, and 0.1 mg/ml of streptomycin. HeLa and COS-7 cells were maintained in DMEM with the same supplements. DEX and cycloheximide (CHX) were purchased from Sigma.

Plasmid construction

To generate pGRE-Luc, the oligonucleotides 5′-TCGATCAGAA CACTGTGTTCTGA-3′ and 5′-TCGATCAGAACACAGTGTTCT GA-3′ were annealed and subcloned into the *Xho*I site of pGV-P2 (Wako Chemicals, Osaka, Japan). Genomic sequences corresponding to human *GZMA*, *FKBP5*, and *DSCR1* were amplified by PCR with appropriate primers using the Expand

Correspondence: Dr T Miyashita, Department of Genetics, National Research Institute for Child Health and Development, 2-10-1 Ohkura, Setagaya-ku, Tokyo 157-8535, Japan; Fax: +81 3 3416 2222;
E-mail: tmiyashita@nch.go.jp
Received 4 June 2004; accepted 3 August 2004; Published online 23 September 2004

High Fidelity PCR system (Roche Diagnostics) and subcloned into a luciferase vector, pGV-B2 or pGV-P2 (Wako Chemicals). Reporter constructs with mutated sequences were generated by the PCR-based method described previously.[16] Detailed information on the primers used for the PCR is available at Leukemia's website. All the constructs were verified by DNA sequencing.

Analysis of gene expression by RT-PCR

To analyze the isoform-specific regulation of *DSCR1*, 500 ng of total RNA extracted from 697 cells was reverse-transcribed and cDNA was amplified by PCR using a forward primer specific to *DSCR1* exon 1 or 4, and a reverse primer for exon 5. Logarithmically amplifying PCR product was subjected to agarose gel electrophoresis. For real-time RT-PCR, one-step RT-PCR was performed using a 7700 ABI PRISM Sequence Detector System (Perkin Elmer-Applied Biosystems). Fluorogenic probes carrying 5′ 6-carboxy-fluorescein as a reporter dye and 3′ 6-carboxy-tetramethyl-rhodamine as a quencher dye were used to detect the PCR product. In every experiment, the *glyceraldehyde-3-phosphate dehydrogenase* (*GAPDH*) gene was amplified using a series of dilutions of a known amount of the standard RNA supplied by Perkin Elmer to prepare a standard curve. Data analysis was performed as described[17] with slight modifications. Detailed information on the primers used for the PCR is available at Leukemia's website.

Western blot analysis

Western blot analysis was performed as described previously[5] using goat anti-FKBP51 polyclonal antibody (F-13, Santa Cruz) followed by horseradish peroxidase-conjugated donkey anti-goat immunoglobulins (Santa Cruz). The proteins were visualized using an enhanced chemiluminescence method (Amersham).

Transfection and luciferase assay

HeLa cells growing in six-well plates were transfected with 750 ng of the reporter gene plasmid along with 500 ng of pCMVβGal and 750 ng of an expression plasmid for rat GR, p6RGR[18] (a gift from Keith Yamamoto), using Effectene reagent (Qiagen). The medium was replaced with DMEM without phenol red (Invitrogen) with 10% charcoal-treated fetal calf serum just before the lipofection. The cells were harvested at 16 h after transfection and used for a luciferase assay. Luciferase activities were measured as described previously and normalized for transfection efficiency based on β-galactosidase activities.[19]

Electrophoretic mobility shift assay

COS-7 cells were transfected with p6RGR and 10^{-6} M of DEX was added. Nuclear extract was prepared 48 h after transfection by three cycles of freezing and thawing in cell resuspension buffer (40 mM HEPES-KOH, pH 7.9, 0.4 M KCl, 1 mM dithiothreitol, 10% glycerol, 0.1 mM phenylmethylsulfonyl fluoride, and 0.1% aprotinin) and incubated with an end-labeled double-stranded oligonucleotide probe: FKBP5 GRE2 5′-AGTAACA CAATGTACAGGTTTGTAGCATTG-3′; GZMA GRE3 5′-TGG GAGAATCCAAGAACATCTGGTGCAGGA-3′; GZMA GRE4 5′-TGTGTTTAGTTCTCACTGTTCC-3′. The reaction was performed in 15 μl of binding buffer (4% glycerol, 1 mM $MgCl_2$, 0.5 mM EDTA, 50 mM NaCl, 10 mM Tris-HCl (pH 7.5), and 0.05 mg/ml poly(dI-dC)) for 20 min at room temperature. The supershift analysis was performed by including anti-GR polyclonal antibody (Affinity Bioreagents) in binding reactions. Samples were fractioned on a nondenaturing 6% polyacrylamide gel and visualized by autoradiography.

Results

Three candidate target genes are upregulated by GC in the absence of de novo *protein synthesis*

We and others have identified *GZMA*, *FKBP5*, and *DSCR1* as GC-responsive genes using microarray technology.[5,20–23] However, it is likely that some of the GC-induced genes identified are regulated because of secondary effects induced by the primary targets of GC. To rule out this possibility, we analyzed the effect of GC in the presence and absence of an inhibitor of protein synthesis, CHX. Evidently, protein synthesis was indeed shut down by CHX as the level of FKBP5 protein declined in cells growing in the presence of CHX even after DEX treatment, in contrast to the experiment without CHX (Figure 1a). Hence, direct target genes of GC will be transcriptionally activated, but because of the inhibition of protein synthesis, the GC-induced proteins will not be synthesized and will not induce secondary

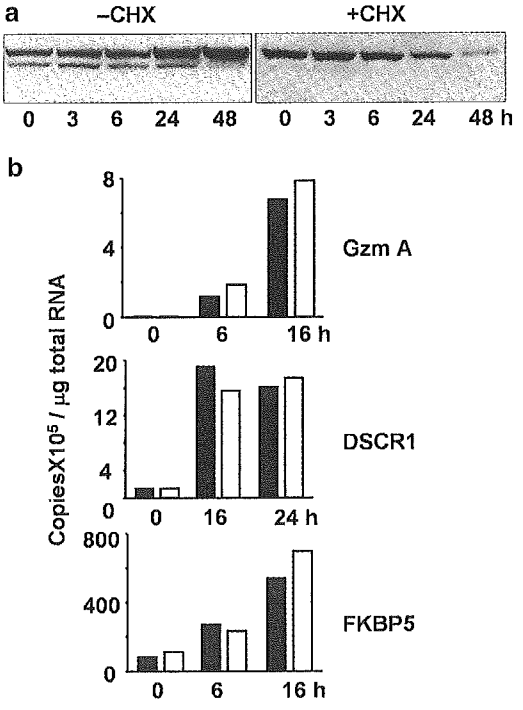

Figure 1 Three genes are directly upregulated by DEX. (a) Cell lysates were obtained from 697 cells treated with 10^{-6} M of DEX for the periods indicated and subjected to Western blotting to detect FKBP5. In some experiments (indicated by +CHX), 10 μg/ml of CHX was added at 16 h prior to DEX treatment. (b) Transactivation of the three genes by DEX is CHX-insensitive. 697 cells growing in the presence (open columns) or absence (closed columns) of CHX for 16 h were treated with DEX for the periods indicated and then total RNA was extracted. cDNA encoding the three genes was amplified by RT-PCR and analyzed with a 7700 ABI PRISM Sequence Detector System. The expression of the genes normalized to that of *GAPDH* is shown. The analysis was performed in triplicate.

or indirect targets in this experimental system. As shown in Figure 1b, these three genes were induced significantly irrespective of the presence of CHX as assessed by real-time RT-PCR, suggesting that their expression was induced directly by GC without the need for protein synthesis.

The exon 1 variant of DSCR1 *is responsive to GC*

The human *DSCR1* gene was reported to express four variant mRNAs with each of four alternative exons (exons 1–4) incorporated selectively at the 5′ terminus of the expressed transcript.[8] The majority of these transcripts were identified to represent isoforms that include exon 1 or 4 (Figure 2a) and the other two were not detectable in human fetal and adult tissues by Northern analysis.[8] Exon 1 and 4 isoforms use distinct promoters and their transcription is differentially regulated. For example, expression of the exon 4 isoform, but not the exon 1 isoform, is selectively increased by calcineurin activity, creating a negative feedback circuit.[24] To address the issue of which variant is responsible for the upregulation of *DSCR1* by GC, we constructed RT-PCR primers that specifically recognize these isoforms (Figure 2a). As shown in Figure 2b, transcription of the exon 1 isoform (Exon1-5) is upregulated by DEX showing a similar time course as total *DSCR1* expression (Exon7-7). However, the exon 4 isoform (Exon4-5) was barely detectable in 697 cells and its expression level was not increased after the treatment with DEX. The exon 4 isoform was detected in the heart and kidney in which this variant was reported to be significantly expressed,[8] demonstrating that these primers were capable of efficiently recognizing the exon 4 isoform (Figure 2c). Collectively, GCs were demonstrated to upregulate the exon 1 isoform of *DSCR1*. Since *DSCR1* spliced from exons 1 and 4 would generate DSCR1 proteins with distinct N-terminus, it would be interesting to see if there is a difference in calcineurin inhibition between these two protein variants.

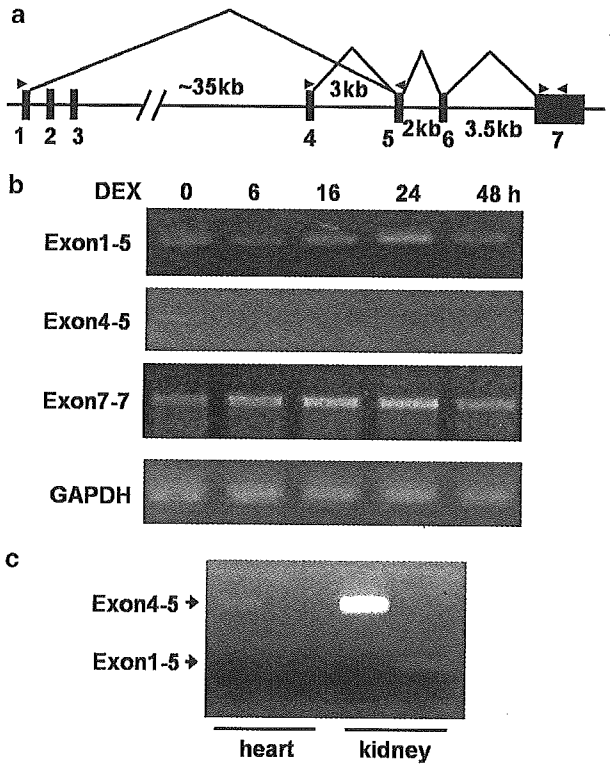

Figure 2 Variant-specific transcriptional regulation of DSCR1. (a) Genomic organization of the human *DSCR1* gene, indicating four alternative initial exons (1–4) and three exons common to all forms of *DSCR1* mRNA (5–7). Locations of two forward primers in initial exons and a reverse primer in exon 5, as well as a pair of primers in exon 7 to detect the total amount of *DSCR1* mRNA are indicated by arrowheads. (b) Semiquantitative RT-PCR analysis to detect *DSCR1*. 697 cells were treated with 10^{-6} M of DEX for the time periods indicated and total RNA was extracted for RT-PCR. Locations of the primers used for RT-PCR are indicated on the left. The *GAPDH* gene was amplified as an internal control. (c) RT-PCR analysis using adult human tissues. RT-PCR was performed similarly except that RNAs from human tissues were used as templates.

Intronic regions of GZMA *and* FKBP5 *are required for a transcriptional response to GC*

Having shown that the expression of the three genes was induced directly by GC, we amplified the promoter and intron fragments from human genomic DNA by PCR and subcloned them into a luciferase vector in order to further substantiate the role of the transcriptional activation of these genes. Despite extensive analysis of the reporter gene, no sequence responsive to GC was identified in the region around exon 1 for *DSCR1* (at least not up to ~2.2 kb and down to ~2.0 kb from exon 1), although a couple of candidate GREs were found in this region (data not shown). These results suggest that the functional GRE is located at a position distant from exon 1 or the transactivation of *DSCR1* is mediated by a nonclassical mechanism.

The *GZMA* promoter was also unresponsive to GC at least up to ~2.3 kb from exon 1 (Figure 3a, pGV-GzmPro). However, when an ~2.7 kb fragment of intron 1 was subcloned into a reporter vector, it was significantly upregulated by DEX (pGV-GzmInt). The degree of induction was more than two-fold that with pGV-GRE in which the consensus 1 × GRE (5′-AGAA CACTGTGTT-3′) was subcloned. To narrow down the region reactive to GC, the 2.7 kb segment was divided into three and various deletion mutants were tested for the response to DEX. As shown in Figure 3b, the response to DEX was completely eliminated when the middle segment of ~1 kb was deleted from the construct (pGV-GzmIntA and pGV-GzmIntC) indicating the presence of a GC-responsive element in this fragment. It was also suggested that the downstream sequence in intron 1 has an inhibitory effect on GC-induced transactivation since the constructs lacking this segment showed significantly higher induction (pGV-GzmIntAB and pGV-GzmIntB). In fact, inspection of the DNA sequence in this middle segment revealed the presence of four candidate GREs that partially match the previously reported consensus sequence (numbered GRE1 to GRE4 as shown in Figure 3c). We therefore introduced a series of nucleotide substitutions at these sites to map the actual GREs. When either GRE3 or GRE4 was mutated, DEX-mediated transactivation was markedly compromised down to less than 10-fold (pGV-GzmIntB3, pGV-GzmIntB4). In addition, their combined mutations virtually eliminated DEX-mediated transactivation (pGV-GzmIntB234, pGV-GzmIntB1234). In contrast, reporter constructs with a mutation of either GRE1 or GRE2 still showed more than 20-fold activation by DEX (pGV-GzmIntB1, pGV-GzmIntB2). These results imply that GRE3 and GRE4 are functional GREs, although GRE1 and GRE2 may have an auxiliary role.

The *FKBP5* gene was similarly examined for the presence of a functional GRE. Again, the promoter sequence of ~2 kb did not respond to the treatment with DEX (Figure 4a, pGV-FKBPPro).

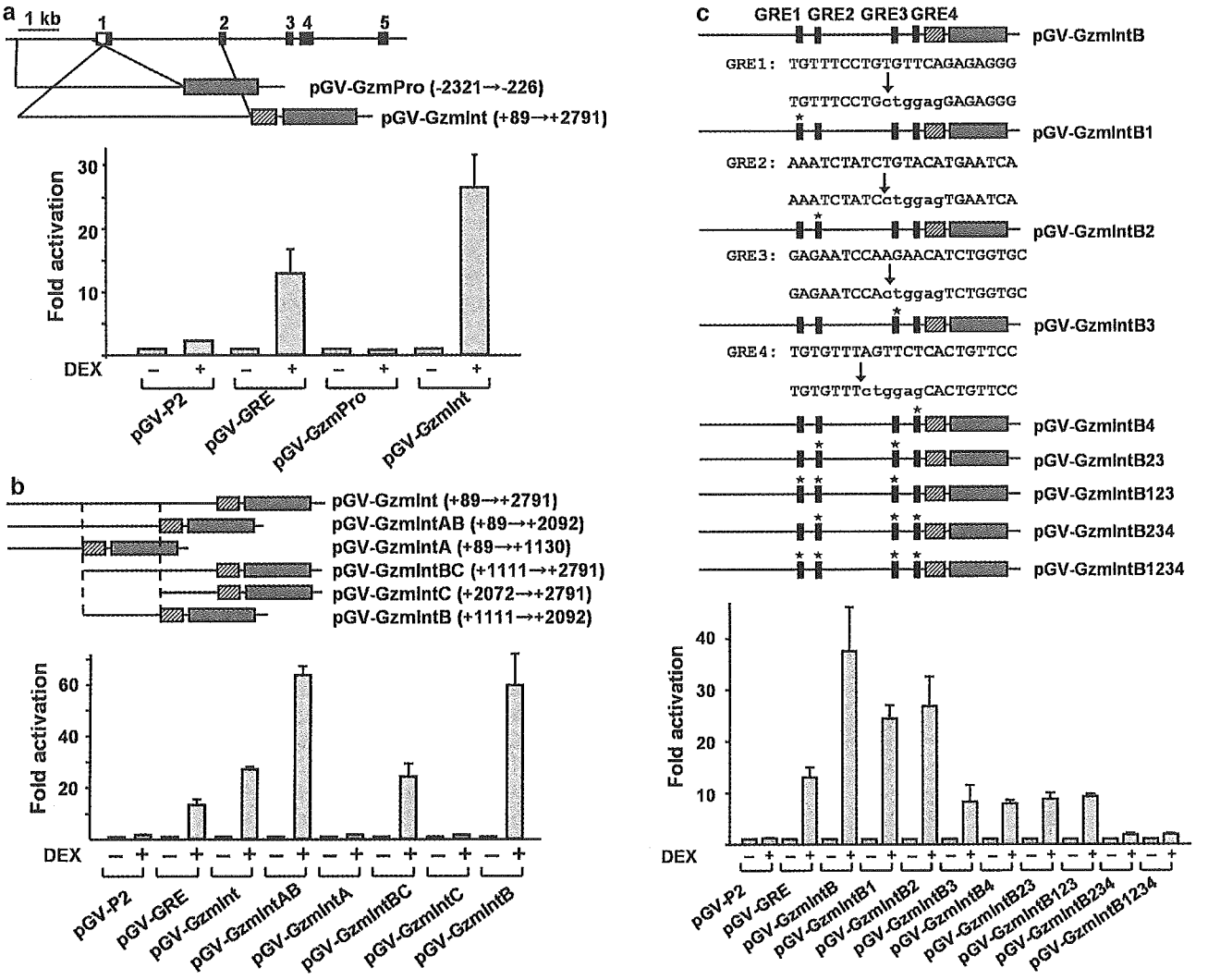

Figure 3 Regulation of the *GZMA* intron by GC. (a) The genomic organization of the human *GZMA* gene and reporter gene constructs used for luciferase assays are schematically depicted at the top. Open and filled boxes indicate noncoding and coding exons, respectively. Striped and gray boxes indicate DNA sequences encoding the SV40 promoter and luciferase, respectively. Numbers in parentheses denote nucleotide positions relative to the translational initiation site based on the genomic sequence, AC091977. Results of transient transfection assays of GZMA-luciferase reporter plasmids are shown in the bottom panel. HeLa cells were transfected with the indicated reporter gene plasmid along with pCMVβGal and p6RGR. The medium was replaced with DMEM containing 10% charcoal-treated fetal calf serum without phenol red (Invitrogen) just before the lipofection. Cells grown in the presence or absence of 10^{-6} M DEX were harvested at 16 h after transfection and used for a luciferase assay. Luciferase activities normalized for β-galactosidase activities were expressed as fold activation. Data are representative of three experiments with similar results. (b) The middle part of intron 1 is GC-responsive. To narrow down the region reactive to DEX, intron 1 was divided into three and subcloned into the reporter vector as depicted in the upper panel. Luciferase assays were performed and expressed as described in (a). (c) Identification of GRE in intron 1. Candidate GRE sequences were mutated as indicated by a PCR-based method. Lowercase letters indicate mutated nucleotides. Thick vertical bars represent the location of candidate GREs. Mutated GREs are marked by asterisks. Luciferase assays were performed and the results were expressed as described in (a).

Since introns 1 and 2 are ~46 and ~5.5 kb long, respectively, we inspected the vicinity of exons 1 and 2 for the presence of possible GREs. Four candidate GREs found in this region were subcloned into a luciferase vector and subjected to reporter gene analyses (Figure 4a). The luciferase constructs containing two candidate GREs in intron 2 (pGV-FKBPIntC) significantly responded to DEX to the same degree as pGV-GRE, whereas the constructs containing the other two candidate GREs in intron 1 were unresponsive to DEX (pGV-FKBPIntA and pGV-FKBPIntB). When the downstream GRE of pGV-FKBPIntC, but not the upstream one, was mutated, the response was virtually eliminated, suggesting that the downstream GRE is functional (Figure 4b, pGV-FKBPIntCmt2).

GR can bind in vitro *to an oligonucleotide probe representing the* GZMA *and* FKBP5 *gene region*

To determine whether the GR protein can bind to the sequences corresponding to the GREs in *GZMA* and *FKBP5* that proved to be functional in reporter gene assays, electrophoretic mobility shift assays were performed. As shown in Figure 5a, when nuclear extracts were obtained from COS-7 cells transiently transfected with expression plasmid for GR and incubated with a radiolabeled DNA probe containing a GRE sequence in the intronic region, a complex with a shift in gel mobility was detected (lanes 1, 4, and 7). When anti-GR antibody was included in binding reactions, the bands detected in the lanes

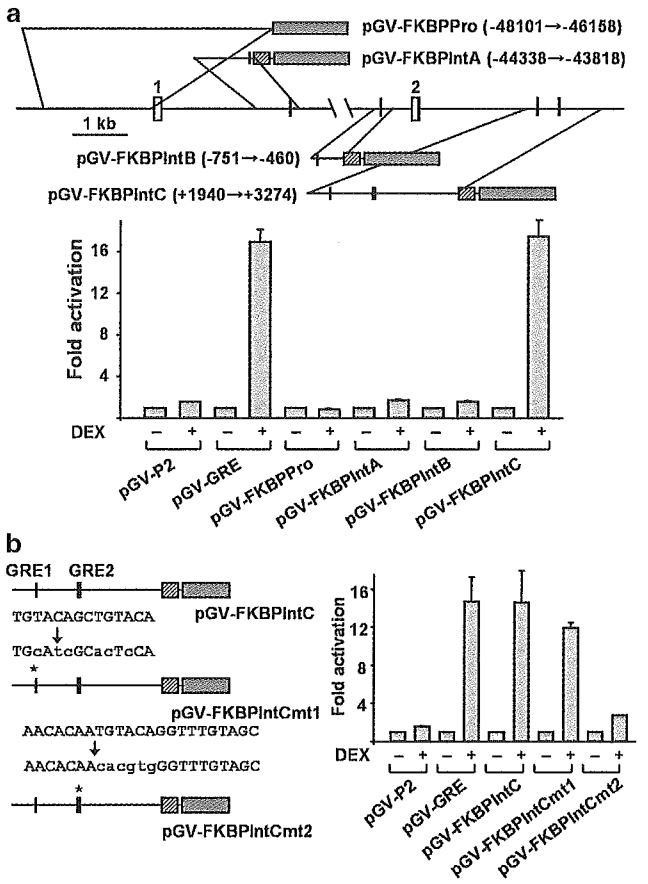

Figure 4 Regulation of the *FKBP5* intron by GC. (a) The genomic organization of the human *FKBP5* gene and reporter gene constructs used for luciferase assays are schematically depicted at the top. Open and filled boxes indicate a noncoding and a coding exon, respectively. Exons 1 and 2 are separated by a sequence ~46 kb long. Numbers in parentheses denote nucleotide positions relative to the translational initiation site in exon 2 based on the genomic sequence, AL033519 and AL590400. Thick vertical bars represent the location of candidate GREs. Luciferase assays were performed and the results were expressed as described in Figure 3. (b) Identification of GRE in intron 2. Candidate GRE sequences were mutated as indicated by a PCR-based method. Lowercase letters indicate mutated nucleotides. Mutated GREs are marked by asterisks. Luciferase assays were performed and the results were expressed as described in Figure 3.

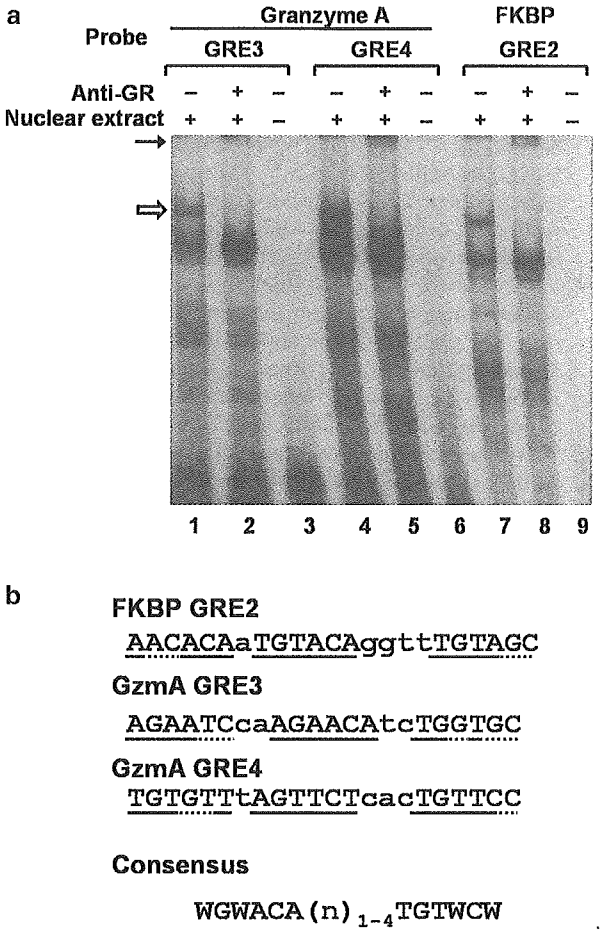

Figure 5 Electrophoretic mobility shift assays and alignment of GC-reactive sequences. (a) GR can bind *in vitro* to an oligonucleotide probe representing the *GZMA* and *FKBP5* gene region. Nuclear extracts were obtained from COS-7 cells transiently transfected with expression plasmid for GR and incubated with ^{32}P-labeled oligonucleotide DNA probes containing putative GRE sequences with or without polyclonal antibody against GR as indicated. DNA–protein complexes were size-fractionated in a nondenaturing polyacrylamide gel and detected by autoradiography. The shifted and supershifted complexes are indicated by open and closed arrows, respectively. (b) DNA sequences demonstrated to be reactive to GC are aligned. The consensus motif deduced from the alignment is indicated at the bottom. Nucleotides that fit and do not fit into the consensus motif are indicated by solid and broken underlines, respectively. Lowercase letters indicate nucleotides that separate 5-bp consensus sequences. W indicates the nucleotide A or T.

mentioned above were replaced by supershifted bands (lanes 2, 5, and 8), demonstrating the specificity of the complex formation. These results indicate that GR binds to the GRE sequences in the *GZMA* and *FKBP5* genes *in vitro*, which were identified by reporter gene assays.

Discussion

Although a number of reports have been published on the genome-wide screening of GC-induced genes,[5,20–23,25] to our knowledge, no reports have dealt with the molecular mechanism of how screened genes are transactivated by GC. Among the genes screened in our previous study, we focused on *GZMA*, *DSCR1*, and *FKBP5*, which have reportedly been relevant to GC-induced apoptosis, and found that all three are direct targets of GC. In the *GZMA* and *FKBP5* genes, GC-responsive intronic sequences to which GR can bind *in vitro* have been determined. None of the promoter sequence we analyzed responded to GC. However, this is not unexpected because a number of transcription factors, for example p53, transactivate target genes by binding to intronic sequences.[26–28] Recently, it was reported that ~400 bp of promoter sequence of human *FKBP5* exhibited upregulation by progestin in human breast cancer cells.[29] In contrast, our reporter construct, which contained this region, was unresponsive to GC, although the receptors for GC and progestin are known to recognize a sequence that is similar, if not the same.[30] Given their findings that no classical progestin-responsive element was identified in this region and the activity of luciferase was stimulated only 2.5-fold by a progesterone analog, much weaker than >10-fold effect observed in our study, it is speculated that progestin mainly regulates the

transcription of *FKBP5* through the intronic sequence we identified rather than a promoter sequence.

The DNA sequences that were responsive to DEX in our study were aligned in Figure 5b. The recognition sequence of GR is defined as a 15-bp motif with partial dyad symmetry such as 5′-GGTACAnnnTGTTCT-3′.[31] However, a mutagenesis study indicated that some sequences that do not perfectly fit into the consensus sequence are still GC-responsive.[30] Based on our results, three repeats of 5′-WGWWCW-3′ separated by 1–4 bp are responsive to GC in which the second motif needs to have a perfect match. However, the presence of this sequence alone does not result in a functional GRE. Indeed, the sequence in *GZMA* that fulfills this consensus sequence, for example GRE2 in Figure 3c, was not functional, because disruption of this candidate GRE had little effect on the response to GC. Therefore, the induction potential of a given site is speculated to be a complex function in the context of the higher gene structure.

The molecular mechanism of GC-induced apoptosis is not fully understood. In the first place, it is necessary for GR to function as a transactivator in order to induce apoptosis, because mutant GR incapable of binding DNA fails to induce thymocyte apoptosis[32] and inhibition of *de novo* protein synthesis by CHX virtually eliminated DEX-induced apoptosis in 697 cells (data not shown). In addition to the genes investigated in this study, the *Bim* gene (*BCL2L11*) has recently been reported to be induced by GC in murine lymphoma cell lines.[25] Bim protein is a BH3-only member of the Bcl-2 family that is capable of directly activating the apoptotic cascade.[33] It is therefore an attractive candidate for a GC target gene that mediates apoptosis. However, at least in our microarray analysis, *Bim* expression was not induced at any time points examined after DEX treatment, although its expression at low levels was observed (data not shown). Thus, we conclude that *Bim* is unlikely a target of GC that generally mediates GC-induced apoptosis. Nevertheless, the levels of *Bim* expression may determine the sensitivity of leukemic cells to GC, since GC-induced apoptosis is partially impaired in hematopoietic cells from $Bim^{-/-}$ mice.[34]

Is one of the genes investigated here solely responsible for GC-induced cell death? We established a lentivirus-mediated small interference RNA delivery system to selectively knock down *FKBP5* or *DSCR1*. The knocking-down of a single gene, however, was not sufficient to significantly inhibit GC-induced apoptosis, suggesting that multiple GR-induced genes activate a network of pathways that contribute to apoptosis (data not shown). This is reminiscent of p53-induced apoptosis. More than 16 target genes of p53 have been proposed to mediate apoptosis, but it is still unclear whether any single target gene is critical. Several lines of evidence suggest that the signaling pathway of p53-induced apoptosis is cell type-dependent and two or more genes cooperate to induce cell death in certain situations.[35,36] In this regard, it should be noted that the *granzyme K* gene, *GZMK*, is also significantly upregulated by GC (data not shown). *GZMK* encodes a serine protease that has features common to granzyme A, and the two genes are only ~70 kb apart on human chromosome 5. Thus, *GZMK* may be another target of GC that mediates apoptosis. Generating mice doubly deficient in GC target genes would help to clarify the signal transduction of GC-induced apoptosis. Expression profiling of the genes described in this study will contribute to predictions of responsiveness or resistance to GC therapy. Further study of GC target genes will provide the rationale for the optimal use of GC to improve treatment outcome in leukemia.

Acknowledgements

We thank Kaori Inoue and Mayu Yamazaki for technical support, Kayoko Saito for preparing the manuscript, and Dr Keith Yamamoto for providing plasmids. This work was supported by Grants for Cancer Research, Genome Research and Child Health and Development from the Ministry of Health, Labour and Welfare; Grant-in-Aid for Scientific Research and the Budget for Nuclear Research from the Ministry of Education, Culture, Sports, Science and Technology, Japan.

Supplementary Information

Supplementary Information accompanies the paper on the Leukemia website (http://www.nature.com/leu).

References

1 Distelhorst CW. Recent insights into the mechanism of glucocorticosteroid-induced apoptosis. *Cell Death Differ* 2002; **9**: 6–19.
2 Tissing WJ, Meijerink JP, den Boer ML, Pieters R. Molecular determinants of glucocorticoid sensitivity and resistance in acute lymphoblastic leukemia. *Leukemia* 2003; **17**: 17–25.
3 Riccardi C, Cifone MG, Migliorati G. Glucocorticoid hormone-induced modulation of gene expression and regulation of T-cell death: role of GITR and GILZ, two dexamethasone-induced genes. *Cell Death Differ* 1999; **6**: 1182–1189.
4 Barker PE, Carroll AJ, Cooper MD. t(1;19)(q23;p13) in pre-B acute lymphocytic leukemia cell line 697. *Cancer Genet Cytogenet* 1987; **25**: 379–380.
5 Yoshida N-L, Miyashita T, U M, Yamada M, Reed JC, Sugita Y *et al.* Analysis of gene expression patterns during glucocorticoid-induced apoptosis using oligonucleotide arrays. *Biochem Biophys Res Commun* 2002; **293**: 1254–1261.
6 Beresford PJ, Kam CM, Powers JC, Lieberman J. Recombinant human granzyme A binds to two putative HLA-associated proteins and cleaves one of them. *Proc Natl Acad Sci USA* 1997; **94**: 9285–9290.
7 Shresta S, Graubert TA, Thomas DA, Raptis SZ, Ley TJ. Granzyme A initiates an alternative pathway for granule-mediated apoptosis. *Immunity* 1999; **10**: 595–605.
8 Fuentes JJ, Pritchard MA, Estivill X. Genomic organization, alternative splicing, and expression patterns of the *DSCR1* (Down syndrome candidate region 1) gene. *Genomics* 1997; **44**: 358–361.
9 Baughman G, Wiederrecht GJ, Campbell NF, Martin MM, Bourgeois S. FKBP51, a novel T-cell-specific immunophilin capable of calcineurin inhibition. *Mol Cell Biol* 1995; **15**: 4395–4402.
10 Vega RB, Yang J, Rothermel BA, Bassel-Duby R, Williams RS. Multiple domains of MCIP1 contribute to inhibition of calcineurin activity. *J Biol Chem* 2002; **277**: 30401–30407.
11 Yamada M, Hirasawa A, Shiojima S, Tsujimoto G. Granzyme A mediates glucocorticoid-induced apoptosis in leukemia cells. *FASEB J* 2003; **17**: 1712–1714.
12 Zhao Y, Tozawa Y, Iseki R, Mukai M, Iwata M. Calcineurin activation protects T cells from glucocorticoid-induced apoptosis. *J Immunol* 1995; **154**: 6346–6354.
13 Asada A, Zhao Y, Kondo S, Iwata M. Induction of thymocyte apoptosis by Ca^{2+}-independent protein kinase C (nPKC) activation and its regulation by calcineurin activation. *J Biol Chem* 1998; **273**: 28392–28398.
14 McEwan IJ, Wright AP, Gustafsson JA. Mechanism of gene expression by the glucocorticoid receptor: role of protein–protein interactions. *BioEssays* 1997; **19**: 153–160.
15 Stöcklin E, Wissler M, Gouilleux F, Groner B. Functional interactions between Stat5 and the glucocorticoid receptor. *Nature* 1996; **383**: 726–728.
16 Imai Y, Matsushima Y, Sugimura T, Terada M. A simple and rapid method for generating a deletion by PCR. *Nucleic Acids Res* 1991; **19**: 2785.

17 Pawlowski V, Revillion F, Hornez L, Peyrat JP. A real-time one-step reverse transcriptase-polymerase chain reaction method to quantify c-erbB-2 expression in human breast cancer. *Cancer Detect Prev* 2000; **24**: 212–223.
18 Miesfeld R, Rusconi S, Godowski PJ, Maler BA, Okret S, Wikstrom AC *et al.* Genetic complementation of a glucocorticoid receptor deficiency by expression of cloned receptor cDNA. *Cell* 1986; **46**: 389–399.
19 Shikama Y, Yamada M, Miyashita T. Caspase-8 and caspase-10 activate NF-κB through RIP, NIK and IKKα kinases. *Eur J Immunol* 2003; **33**: 1998–2006.
20 Galon J, Franchimont D, Hiroi N, Frey G, Boettner A, Ehrhart-Bornstein M *et al.* Gene profiling reveals unknown enhancing and suppressive actions of glucocorticoids on immune cells. *FASEB J* 2002; **16**: 61–71.
21 Planey SL, Abrams MT, Robertson NM, Litwack G. Role of apical caspases and glucocorticoid-regulated genes in glucocorticoid-induced apoptosis of pre-B leukemic cells. *Cancer Res* 2003; **63**: 172–178.
22 Tonko M, Ausserlechner MJ, Bernhard D, Helmberg A, Kofler R. Gene expression profiles of proliferating *vs* G1/G0 arrested human leukemia cells suggest a mechanism for glucocorticoid-induced apoptosis. *FASEB J* 2001; **15**: 693–699.
23 Chauhan D, Auclair D, Robinson EK, Hideshima T, Li G, Podar K *et al.* Identification of genes regulated by dexamethasone in multiple myeloma cells using oligonucleotide arrays. *Oncogene* 2002; **21**: 1346–1358.
24 Yang J, Rothermel B, Vega RB, Frey N, McKinsey TA, Olson EN *et al.* Independent signals control expression of the calcineurin inhibitory proteins MCIP1 and MCIP2 in striated muscles. *Circ Res* 2000; **87**: E61–E68.
25 Wang Z, Malone MH, He H, McColl KS, Distelhorst CW. Microarray analysis uncovers the induction of the proapoptotic BH3-only protein Bim in multiple models of glucocorticoid-induced apoptosis. *J Biol Chem* 2003; **278**: 23861–23867.
26 Kastan MB, Zhan Q, el Deiry WS, Carrier F, Jacks T, Walsh WV *et al.* A mammalian cell cycle checkpoint pathway utilizing p53 and *GADD45* is defective in ataxia-telangiectasia. *Cell* 1992; **71**: 587–597.
27 Oda K, Arakawa H, Tanaka T, Matsuda K, Tanikawa C, Mori T *et al. p53AIP1*, a potential mediator of p53-dependent apoptosis, and its regulation by Ser-46-phosphorylated p53. *Cell* 2000; **102**: 849–862.
28 de Stanchina E, Querido E, Narita M, Davuluri RV, Pandolfi PP, Ferbeyre G *et al.* PML is a direct p53 target that modulates p53 effector functions. *Mol Cell* 2004; **13**: 523–535.
29 Hubler TR, Denny WB, Valentine DL, Cheung-Flynn J, Smith DF, Scammell JG. The FK506-binding immunophilin FKBP51 is transcriptionally regulated by progestin and attenuates progestin responsiveness. *Endocrinology* 2003; **144**: 2380–2387.
30 Strähle U, Klock G, Schütz G. A DNA sequence of 15 base pairs is sufficient to mediate both glucocorticoid and progesterone induction of gene expression. *Proc Natl Acad Sci USA* 1987; **84**: 7871–7875.
31 Beato M, Chalepakis G, Schauer M, Slater EP. DNA regulatory elements for steroid hormones. *J Steroid Biochem* 1989; **32**: 737–747.
32 Reichardt HM, Kaestner KH, Tuckermann J, Kretz O, Wessely O, Bock R *et al.* DNA binding of the glucocorticoid receptor is not essential for survival. *Cell* 1998; **93**: 531–541.
33 O'Connor L, Strasser A, O'Reilly LA, Hausmann G, Adams JM, Cory S *et al.* Bim: a novel member of the Bcl-2 family that promotes apoptosis. *EMBO J* 1998; **17**: 384–395.
34 Bouillet P, Metcalf D, Huang DC, Tarlinton DM, Kay TW, Kontgen F *et al.* Proapoptotic Bcl-2 relative Bim required for certain apoptotic responses, leukocyte homeostasis, and to preclude autoimmunity. *Science* 1999; **286**: 1735–1738.
35 Lindsten T, Ross AJ, King A, Zong WX, Rathmell JC, Shiels HA *et al.* The combined functions of proapoptotic Bcl-2 family members bak and bax are essential for normal development of multiple tissues. *Mol Cell* 2000; **6**: 1389–1399.
36 Villunger A, Michalak EM, Coultas L, Müllauer F, Böck G, Ausserlechner MJ *et al.* p53- and drug-induced apoptotic responses mediated by BH3-only proteins puma and noxa. *Science* 2003; **302**: 1036–1038.

Purification, Molecular Cloning, and Expression of a Novel Growth-Promoting Factor for Retinal Pigment Epithelial Cells, REF-1/TFPI-2

Yasuhiko Tanaka,[1] Jun Utsumi,[2] Mizuo Matsui,[3] Tetsuo Sudo,[2] Noriko Nakamura,[2] Masato Mutoh,[2] Akemi Kajita,[2] Saburo Sone,[2] Kazuteru Kigasawa,[4] Masahiko Shibuya,[1] Venkat N. Reddy,[5] Qiang Zhang,[1,6] and Takeshi Iwata[1]

Purpose. Retinal pigment epithelial (RPE) cells are known to play important roles in maintaining the homeostasis of the retina and in controlling choroidal neovascularization. The purpose of this study was to identify a factor or factors that would stimulate RPE cells to proliferate.

Methods. To isolate such a factor, 100 L of human-fibroblast-conditioned medium underwent ion-exchange, hydrophobic, and reverse-phase chromatographies followed by sodium dodecyl sulfate–polyacrylamide gel electrophoresis. The growth-promoting activity of the factor was examined in a human K-1034 RPE cell line and human primary RPE cells.

Results. The different chromatographic processes isolated a 31-kDa factor that had RPE cell growth–promoting properties. This factor, which we have named RPE cell factor (REF)-1, promotes growth of RPE cells but not of human umbilical vein endothelial cells (HUVECs). The amino-terminal sequence and molecular cloned cDNA of REF-1 were identical with those of tissue-factor pathway inhibitor (TFPI)-2, a family of TFPIs, and placental protein (PP)-5, a serine protease inhibitor. The cDNA expression of REF-1/TFPI-2 with pcDL-pSRα vector in Chinese hamster ovary (CHO) cells confirmed the growth-promoting activity for RPE cells. The major component of the recombinant REF-1/TFPI-2 expressed in CHO cells had a molecular mass of 31 kDa and exerted growth-promoting activity in RPE cells but not in human endothelial cells and fibroblasts in vitro. REF-1/TFPI-2 also had protease inhibitory activity. The other family factor, TFPI-1, did not promote RPE cell growth.

Conclusions. REF-1/TFPI-2 is a novel growth-promoting factor for RPE cells but not for endothelial cells and fibroblasts. Its properties make it potentially beneficial for intraocular therapy for the repair and maintenance of RPE cells. (*Invest Ophthalmol Vis Sci.* 2004;45:245–252) DOI:10.1167/iovs.03-0230

Recent advances in basic and clinical research have shown that the pathogenesis of many retinal and choroidal diseases is closely related to the normal functioning of retinal pigment epithelial (RPE) cells. RPE cells play critical roles in maintaining the homeostasis of the retina and in controlling choroidal neovascularization.[1] Because the denaturation of cellular proteins in the RPE and the loss of function of RPE cells are responsible for retinal and choroidal diseases, a factor that stimulates RPE cell growth could prove to be valuable for the treatment of RPE-related ocular diseases.

At present, various cell growth factors, such as basic fibroblast growth factor (bFGF) and platelet-derived growth factor (PDGF), are known to stimulate the proliferation of RPE cells.[2–4] However, these factors are also known to affect the growth of vascular endothelial cells and fibroblasts,[5–7] and ocular neovascularization and fibroblast proliferation can lead to serious retinal and choroidal diseases and proliferative vitreoretinopathy.

The purpose of this study was to isolate and characterize a factor or factors that would promote RPE cell proliferation. We focused on the supernatant of cultured human fibroblasts as a source of the target factor, because fibroblasts function as stromal cells that are known to produce various cytokines. We have isolated a 31-kDa factor from the conditioned medium of human fibroblasts that promotes growth in RPE cells and named it RPE cell factor (REF)-1. The amino terminal sequence was determined, and molecular cloning of its cDNA showed that the factor was identical with tissue-factor pathway inhibitor (TFPI)-2[8]-placental protein 5 (PP5).[9]

Materials and Methods

Isolation of RPE Cell Growth–Promoting Factor

Human fibroblast DIP-2 cells[10] were cultured for 5 days in Eagle's minimum essential medium (MEM) supplemented with 5% fetal calf serum (FCS) in microcarriers (Cytodex 1; Amersham Biosciences, Tokyo, Japan) in 16-L glass culture vessels at 37°C. After the addition of 100 IU/mL human interferon-β (Toray Industries, Tokyo, Japan) as a priming agent and 10 μg/mL poly(I) poly(C) (Yamasa Shouyu, Choushi, Japan) as a cytokine-inducing reagent, the culture media was replaced by serum-free Eagle's MEM and cultured at 37°C for six additional days.

The cultured medium was collected and filtered to remove the cellular debris. Fractionation was started by passing 100 L of the cultured medium through an S-Sepharose column (500 mL; Amersham Biosciences), and the fraction containing growth-promoting activity (active fraction) was eluted with 200 mL of 10 mM phosphate-buffered

From the [1]National Institute of Sensory Organs, National Tokyo Medical Center, Tokyo, Japan; the [2]Pharmaceutical Research Laboratories, Toray Industries, Inc., Kamakura, Japan; the [3]Department of Ophthalmology, Nihon University Surugadai Hospital, Tokyo, Japan; the [4]Department of Ophthalmology, Tokai University School of Medicine, Isehara, Japan; the [5]Department of Ophthalmology, Kellogg Eye Center, University of Michigan, Ann Arbor, Michigan; and the [6]Department of Ophthalmology, Keio University School of Medicine, Tokyo, Japan.

Supported in part by grants for Research on Sensory and Communicative Disorders by the Ministry of Health, Labor and Welfare, Japan and by National Eye Institute Grants EY00484 and EY07003.

Submitted for publication March 5, 2003; revised September 1, 2003; accepted September 4, 2003.

Disclosure: **Y. Tanaka**, None; **J. Utsumi**, Toray Industries (F, E, P); **M. Matsui**, None; **T. Sudo**, Toray Industries (F, E); **N. Nakamura**, Toray Industries (F, E); **M. Mutoh**, Toray Industries (F, C, P); **A. Kajita**, Toray Industries (F, E); **S. Sone**, Toray Industries (F, E); **K. Kigasawa**, None; **M. Shibuya**, None; **V.N. Reddy**, None; **Q. Zhang**, None; **T. Iwata**, None

The publication costs of this article were defrayed in part by page charge payment. This article must therefore be marked "*advertisement*" in accordance with 18 U.S.C. §1734 solely to indicate this fact.

Corresponding author: Yasuhiko Tanaka, National Institute of Sensory Organs, National Tokyo Medical Center, 2-5-1 Higashigaoka, Meguro-ku, Tokyo 152-8902, Japan; ytanaka@ntmc.hosp.go.jp.

saline (PBS) at pH 7.4 with 0.5 M NaCl. The eluate was added to 1 M ammonium sulfate and applied to a polypropyl A column (0.8 × 25 cm; PolyLC, Columbia, MD). The active protein was eluted by a gradient of 0 to 1 M ammonium sulfate in 10 mM PBS. Four milliliters of the active fraction from the polypropyl A column were injected into a C4 reverse-phase column (1 × 25 cm; Grace Vydac, Hesperia, CA), and the protein was eluted by a gradient of water-acetonitrile (0%–70%) including 0.1% trifluoroacetic acid (TFA; pH 2.0). Two milliliters of the active fraction eluted from the column was concentrated to 100 μL by speed vacuum concentrator (Speed Vac Systems, Savant, MN) and applied to sodium dodecyl sulfate–polyacrylamide gel electrophoresis (SDS-PAGE) under nonreducing conditions without 2-mercaptoethanol (2ME). Immediately after migration of the sample into the gel, the SDS-PAGE gel was cut into 1 × 2 × 4-mm slices and immersed overnight at 4°C in 0.5 mL per slice of distilled water to extract the active protein. The extracted protein was reapplied to SDS-PAGE under reducing–nonreducing conditions to examine the purity and the molecular weight of the target protein.

Determination of Cell Growth–Promoting Activity during Purification

Human K-1034 RPE cells or fourth-passage human primary RPE cells were used to determine RPE cell growth-promoting activity.[11] K-1034 cells or human primary RPE cells were added to collagen type I–coated 24-well plastic plates (Corning International, Tokyo, Japan) at a density of 1 × 10^4 cells/well. DMEM supplemented with 5% FCS (Invitrogen Japan, Tokyo, Japan) or 15% FCS (Invitrogen) was used for K-1034 or human primary RPE cells, respectively. Two microliters of purified REF-1 was added to each well and cultured at 37°C for 5 days. The number of RPE cells at each time point was determined by a cell counter (model ZM; Beckman Coulter K. K., Tokyo, Japan). The growth-promoting rate was calculated as a percentage of the control (n = 4 or 6). In the first exploratory purification, the specific concentration of REF-1 was not determined, as an REF-1 ELISA kit is not available, and REF-1 was therefore traced by the growth-promoting activity in RPE cells.

Determination of Cell Growth–Promoting Activity Using Purified REF-1 Protein

To examine whether purified REF-1 promotes growth in the number of vascular endothelial cells, cells were isolated from the human umbilical vein of a patient at an obstetric hospital. In accordance with the provisions of the Declaration of Helsinki, all subjects signed an informed consent after an explanation of the procedures to be used and the purpose of the studies. The human umbilical vein endothelial cells (HUVECs) were treated under conditions similar to those used for RPE cells (n = 4 or 6). Human fibroblasts (DIP-2 cells), rabbit primary RPE cells, and human primary RPE cells were also used to characterize the growth-promoting activity (n = 6).

A comparison of the growth-promoting profile of other related factors, such as TFPI-1 (American Diagnostica, Greenwich, CT), the family of TFPIs, ciliary neurotrophic factor (CNTF; R&D Systems, Minneapolis, MN), and bFGF (R&D Systems), was performed at a concentration of 10 ng/mL (n = 6).

Amino Acid Analyses of REF-1/TFPI-2

REF-1 was isolated as a 31 ± 3-kDa protein on SDS-PAGE gel under nonreducing conditions. The active fraction appeared to correspond to a single band on the silver-stained gel. REF-1 was isolated from the band and subjected to amino-terminal amino acid sequence analysis (Protein sequencer model 470; Applied Biosystems Japan, Tokyo, Japan).

Amino acid composition analysis of REF-1 component was performed after hydrolysis at 110°C for 22 and 72 hours in 6 M HCl with 4% thioglycolic acid (amino acid analyzer model 835; Hitachi, Tokyo, Japan).

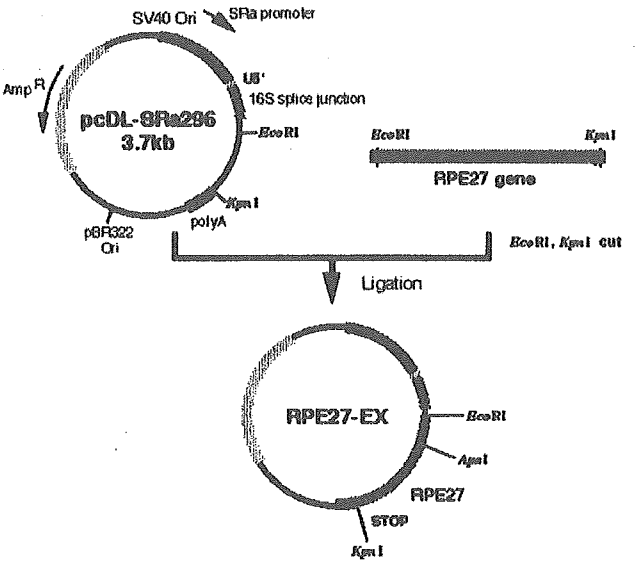

FIGURE 1. The construction of the REF-1 expression vector. The RPE27-EX1 expression vector was obtained by ligation with pcDL-SRα296 vector (3.7 kb) and RPE27 gene (750 bp).

Molecular Cloning of REF-1 Protein

The primers, R1: 5′-GGAAGAAGGCACATGGC-3′, R2: 5′-TATGGGGATTGGTGGCG-3′, R3: 5′-ACTCCTGGAGCCCGTC-3′, L1: 5′-AGACATGGCCTGCCCG-3′, L2: 5′-GACACCAGACCAACTGG-3′, and L3: 5′-GGTAGCGACCGGCGC-3′ were used for PCR amplification of phage insert and were designed based on the sequence of cloning vector λgt11 (Human placenta cDNA library, CLHL1008b; BD Biosciences-Clontech Japan, Tokyo, Japan). The first PCR was performed with primers, R1 and L1, designed to flank the insert of λgt11. The second PCR was performed using 1 μL of the first PCR reaction mixture as template with three primers: 27S1 (5′-GATGCIGAACAAGAACCIACIG-3′) and the R2 and L2 primers. The third PCR was performed with the second PCR mixture as a template, with primer 27S2 (5′-CAAGAACCIACIG-GIACIAATGC-3′) and the R3 and L3 primers.

The PCR conditions were initiated at 94°C for 5 minutes, then 25 cycles at 94°C for 30 seconds, 56°C for 2 minutes, and 72°C for 8 minutes, followed by 1 cycle at 72°C for 7 minutes. The amplified DNA fragment from the third PCR was separated by 1% agarose gel electrophoresis and the DNA fragment was purified from gel by the electroelution method. Purified DNA fragment was cloned using a kit (Sure Clone; Amersham Bioscience). The nucleotide sequence was determined for 16 clones containing full-length cDNA on a DNA sequencer (model 373A; Applied Biosystems).

Construction of Expression Vector for REF-1/TFPI-2

REF-1 cDNA was reamplified by PCR from an original λgt11 phage clone by primer set RPE27-EX1 (5′-GGGGAATTCCTTTCTCGGACGGCTTGC-3′) and RPE27-EX2 (5′-GGGGGTACCTAAAAATTGCTTCTTCCG-3′) to obtain the insert for the expression vector. PCR was performed for 25 cycles in a reaction mixture with 0.2 μg of λgt11 DNA, 1.6 mM dNTP, 1.0 μM of primers (RPE 27-EX1 and RPE 27-EX2), and DNA polymerase (Ex *Taq*; Takara, Tokyo, Japan). The PCR product was digested with *Eco*RI and *Kpn*I and ligated into expression vector pcDL-SRα296 to obtain expression vector RPE27-EX (Fig. 1).[12]

Expression of Recombinant REF-1/TFPI-2 by CHO Cells

The expression vector RPE27-EX and the expression vector pAdDHFR containing dihydrofolate reductase (DHFR) cDNA were cotransfected

into the DHFR gene-deficient CHO DXB11 cell strain. The surviving DHFR-positive cells were selected in αMEM without ribonucleosides and deoxyribonucleosides with 10% FCS. Highly producible cells were then selected by addition of methotrexate (MTX) to the medium. The concentration was increased stepwise from 0.0025 μM, to 0.05 μM, and finally to 1 μM, to obtain highly producible cells.[12]

After reaching confluence, the culture medium was replaced by serum-free αMEM and the medium was collected every 2 days, nine times. The collected medium was centrifuged at 6000 rpm at 4°C for 15 minutes, filtered, and stored at 4°C until the large-scale purification procedures.

Preparation of Anti-REF-1/TFPI-2 Antibody and ELISA

Peptide antibody for REF-1/TFPI-2 was generated, using peptide NH_2-SGGCHRNRIENRFPDE-COOH, corresponding to residues 106-120 as an antigen. Rabbit antiserum was purified on a protein A column (Prosep A; Amersham Biosciences). A sandwich ELISA system was constructed by using primary antibody (5 μg/mL) generated against whole REF-1 protein, biotinylated secondary peptide antibody (5.2 μg/mL) raised against amino acids 106 through 120, and the avidin HRP anti-rabbit antibody. During the process of REF-1 purification, protein quantification was determined by this ELISA kit with detection sensitivity of 10 ng/mL.

Purification of CHO Cell–Derived Recombinant REF-1/TFPI-2

Forty liters of culture supernatant was applied to a gel filtration column (S-Sepharose FF, 5 × 15 cm, 300 mL; Amersham Biosciences) at 2.4 L/h and the column was washed with 1.2 L of 20 mM sodium citrate buffer (pH 5.0) and 1.7 L of buffer containing 0.2 M NaCl. Protein was eluted by 20 mM sodium citrate (pH 5.0)/0.4 M NaCl. TFA was added to the eluate at a final concentration of 0.1% and further purified by reverse-phase chromatography (Resource RPC column, 0.46 × 10 cm, 3 mL; Amersham Biosciences). The elution was performed with acetonitrile gradient of 0% to 70% in 0.1% TFA (pH 2.0). REF-1 was eluted in 19 mL of 31% to 35% acetonitrile fraction. This fraction was diluted with 40 mM PBS (pH 7.2) to twofold volume and applied to a gel filtration column (SP-Sepharose FF, 1 × 1.3 cm, 1 mL; Amersham Biosciences). REF-1 was eluted with 20 mM PBS (pH 7.2) containing 0.45 M NaCl.

Determination of Protease Inhibitor Activity

Plasmin inhibition by REF-1 was analyzed by a method introduced previously.[13] Reaction buffer (50 mM Tris-HCl [pH 7.5], 5 mM $CaCl_2$, 0.1 M NaCl, 0.01% Tween 20) was added to 96-well plastic plates followed by the addition of 0.4 μg aprotinin (Boehringer-Yamanouchi, Tokyo, Japan) and REF-1/TFPI-2 at final concentration of 5 μg/mL. One hundred twenty-five nanograms of plasmin was added (Chromogenix, Milano, Italy) and incubated at room temperature for 30 minutes. Fifty microliters of substrate S-2251 (Val-Leu-Lys-pNA, 1 mg/mL; Chromogenix) was added and the absorbance was measured at 405 to 450 nm for 15 minutes with a microplate photometer (UV/Visible Spectrometer DU640; Beckman Coulter, Fullerton, CA) every 20 seconds. The percentage of relative activity in the inhibitor concentration was then calculated.

Determination of RPE Cell Production of Cytokines

The relationship between RPE cell growth and production of the growth factor bFGF, transforming growth factor (TGF)-β1, transforming growth factor (TGF)-β2, epidermal growth factor (EGF), granulocyte colony-stimulating factor (G-CSF), granulocyte-macrophage CSF (GM-CSF), and macrophage-CSF (M-CSF), and the cytokines interleukin (IL)-1α, IL-6, IL-8, tumor necrosis factor (TNF)-α by human primary RPE cells was examined. The cells were grown in DMEM with 15% FCS for 3 days and the medium then replaced by serum-free DMEM. The cytokines in the culture supernatant were determined for two additional days by ELISA kits (Amersham International, Buckinghamshire, UK; R&D Systems, Minneapolis, MN; Immuno-Biological Laboratories, Gunma, Japan).

Western Blot Analysis of REF-1 for RPE Cell Extract

Cellular extract was obtained from RPE cells by using M-PER (Pierce, Rockford, IL) detergent mixture. A sample amount of 7.2 μg was

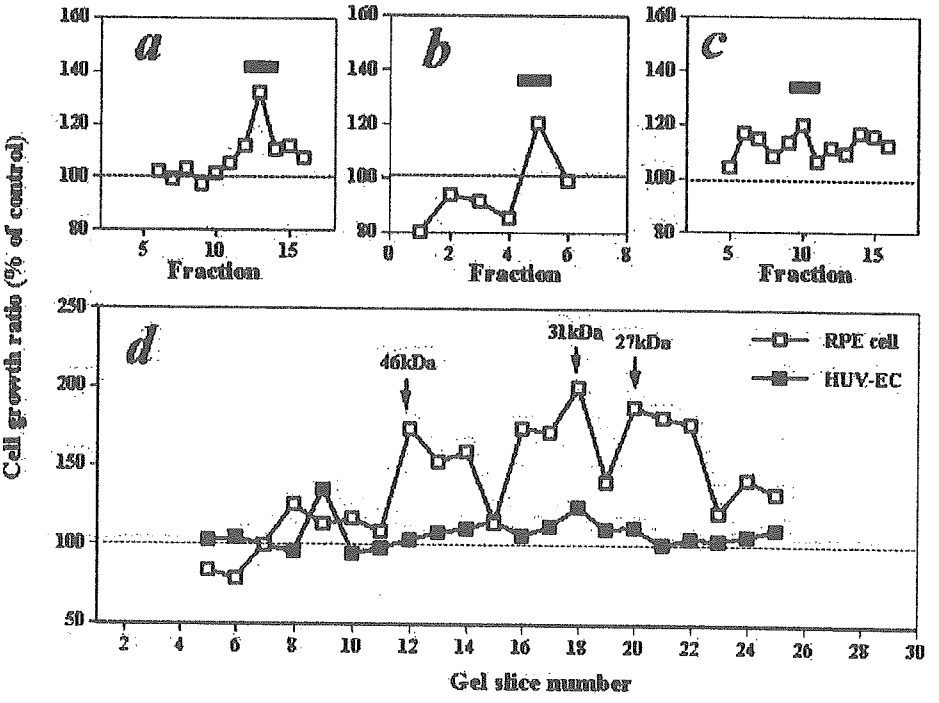

FIGURE 2. Chromatography was used to determine RPE cell growth-promoting activity. Profiles of the activity on S-Sepharose (**a**), polypropyl-A (**b**), and Vydac-C4 (**c**) columns and on a nonreducing SDS-PAGE gel (**d**). Data denote active fractions collected. In the SDS-PAGE fraction, the growth-promoting activity was examined in RPE cells and HUVECs.

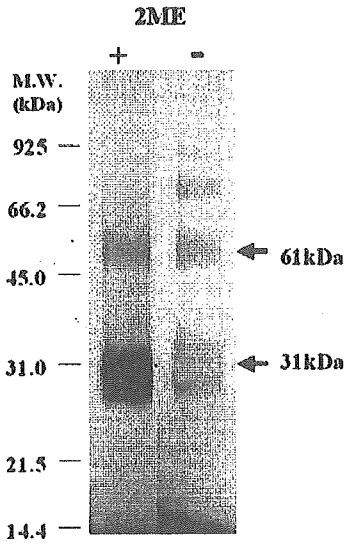

FIGURE 3. SDS-PAGE pattern of the RPE cell growth-promoting factor REF-1 isolated from the conditioned medium of human fibroblasts. Approximately 1 μg/lane of the purified protein was loaded and made visible with silver staining after electrophoresis under reducing (+2ME) and nonreducing (−2ME) conditions. A major band at 31 kDa and a minor band at 61 kDa correspond to the monomeric and dimeric forms of REF-1, respectively.

applied to each lane in 12% polyacrylamide gels. For positive control, bacteria expressing REF-1 protein was added (see Fig. 7, lane 4). After the separation, proteins were transferred to a nitrocellulose membrane (Schleicher & Schuell, Rellichausen, Germany), blocked for 1 hour with the blocking solution containing 10% milk diluent-blocking solution (KPL, Gaithersburg, MD) and 0.1% Tween-20 in phosphate-buffered saline (pH 7.4). The membrane was probed with a rabbit polyclonal anti-REF-1 antibody (1 μg/mL). The specific signal was detected by incubation of anti-rabbit IgG HRP secondary antibody (New England BioLabs, Beverly, MA) followed by chemiluminescence reactions with luminol reagent A and peroxide reagent B, as recommended by the manufacturer (New England BioLabs) and made visible with a chemiluminescence imager (Lumi-Imager F1; Roche Applied Science, Tokyo, Japan).

RNA Isolation from RPE cells and RT-PCR of REF-1

Total RNA was isolated from cultured fourth-passage human primary RPE cells with a total RNA isolation kit (RNA-Bee-RNA Isolation Reagent; Tel-Test, Friendswood, TX). Total RNA samples were digested by RNase-free DNase (Roche Diagnostics Japan) to minimize the risk of genomic DNA contamination. First-strand cDNA was synthesized using random primers (SuperScript First-Strand Synthesis System for RT-PCR; Invitrogen Japan). PCR was performed using 1 μg of single-strand cDNA with 2.5U *Taq* DNA polymerase in a volume of 50 μL. After predenaturation at 95°C for 5 minutes, 30 cycles were performed, including denaturation at 95°C for 30 seconds, annealing at 65°C for 30 seconds, and extension at 72°C for 1 minute, followed by 1% agarose gel electrophoresis. The primers used were: 5′-ATTCTGCTGCTTTTC-CTGAC-3′ (sense primer) and 5′-CAGCTCTGCGTGTACCTGTC-3′ (antisense primer).

RESULTS

Isolation and Identification of an RPE Cell Growth–Promoting Factor

The RPE cell growth-promoting fraction was purified from 100 L of starting material to 0.5 mL of SDS-PAGE gel extract. REF-1 was concentrated by 2×10^5-fold after the final step of purification. The profile of the RPE cell growth-promoting factor is shown at each step in Figure 2. The peak of RPE cell growth promotion was mainly detected in three fractions of molecular mass 46 ± 3, 31 ± 3, and 27 ± 3 kDa on the SDS-PAGE gel. The 31-kDa fraction had the highest RPE cell growth-promoting effect. This fraction showed very low growth stimulation in HUVECs for all molecular sizes detected. The 31-kDa active fraction was separated from the SDS-PAGE gel under reducing-nonreducing conditions. The 31-kDa band was made visible as a major component by silver staining (Fig. 3). There was a minor component at 61 kDa that was predicted as a dimeric form of REF-1. Amino-terminal sequence analysis was performed on the purified 31-kDa protein.

Amino-Terminal Sequence of RPE Cell Growth–Promoting Factor

Amino-terminal sequence analysis of the 31-kDa component resulted in the following sequence: NH_2-Asp-Ala-Glu-Gln-Pro-Thr-Gly-Thr-Asn-Ala-Glu-Ile-Xaa-Ala-COOH (14 amino acids).

In addition, amino-terminal sequence analysis of the 27-kDa component gave nine residues of sequences identical with the 31-kDa component. The polypeptide was named REF-1. Because the amino-terminal sequence of REF-1 was apparently identical with TFPI-2^8-PP5,[9] molecular cloning of REF-1 was performed to confirm the whole sequence of the 31-kDa protein. For the 46-kDa active component isolated on SDS-PAGE gel, the amino acid sequence could not be identified because of insufficient quantity of the protein.

Molecular Cloning of REF-1

Although REF-1 was identical with TFPI-2 at the amino-terminal, molecular cloning was performed to determine the complete cDNA of REF-1. One of the 16 clones isolated had an amino-terminal sequence identical with that of TFPI-2. The cloned REF-1 molecule consisted of 235 amino acids, and the theoretical molecular mass of this polypeptide was 27 kDa. The position of three tandemly arranged Kunitz-type domains and two binding sites of predicted asparagine-linked sugar chains were identical with TFPI-2. From the available evidence, we concluded that REF-1 is identical with TFPI-2. The calculated molecular mass increased by 4 to 6 kDa after possible glycosylation to molecular mass between 31 and 33 kDa.

TABLE 1. Purification of CHO-Cell-Derived Recombinant REF-1

Purification Step	Volume (mL)	Protein Conc (μg/mL)	Total Protein (mg)	REF-1 (mg)	Yield (%)	Purity (%)	Purification (×)
CHO cell CM	40,000.0	113.8	4552.0	10.8	100	0.24	1
S-Sepharose	800.0	82.8	66.2	8.6	80	13.00	54
Resouce RPC	40.0	159.0	6.4	6.4	59	87.00	360
SP-Sepharose	4.2	913.0	3.8	3.8	35	97.00	400

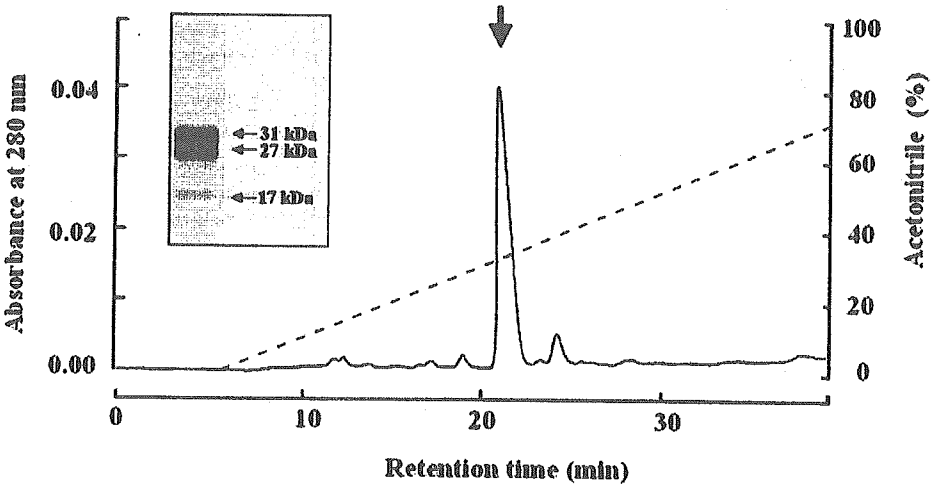

FIGURE 4. Reverse-phase chromatographic profile of CHO-cell-derived recombinant REF-1 in a final purification step. SDS-PAGE was used to amplify recombinant REF-1. Approximately 5 μg of the purified protein was loaded and made visible with Coomassie blue R-250 staining after electrophoresis under reducing (+2ME) conditions. Major components at 31 and 27 kDa and a minor component at 17 kDa were observed.

Purification of CHO Cell–Derived Recombinant REF-1

We developed a large-scale purification procedure for CHO cell-derived recombinant REF-1. From 40 L of conditioned medium of recombinant REF-1-CHO cells, recombinant REF-1 was purified by the combination of cation exchange chromatography and reverse-phase high-performance liquid chromatography (HPLC) as shown in Table 1. The purity of the final recombinant REF-1 was more than 97% on SDS-PAGE gel and was free of pyrogen. The reverse-phase HPLC profile and SDS-PAGE pattern of purified CHO cell-derived recombinant REF-1 are shown in Figure 4.

Molecular Heterogeneity of REF-1

A molecular heterogeneity of the CHO-cell-derived recombinant REF-1 was observed. Three forms of REF-1 at molecular masses of 31 ± 1, 27 ± 1, and 17 ± 1 kDa were found. The ratios for each size were approximately 40% for 31 kDa, 50% for 27 kDa, and 10% for 17 kDa. The 31- and 27-kDa components were major and appeared to be different because of attached sugar chains. The 17-kDa component was smaller than the theoretical molecular mass by approximately 10 kDa. This form was possibly produced by extracellular protease digestion after the secretion of the mature form based on the amino acid composition analysis. The molecular mass of 10 kDa was calculated to match the 28-kDa component lacking the C-terminal portion.

Currently, data are not available for the differences in biological effects of the different molecular forms. TFPI-2 also demonstrated molecular heterogeneity of 31 and 27 kDa, and it has been suggested that this may be due to different glycosylated forms.[14]

Cell Growth–Promoting Activity of Recombinant REF-1

The growth-promoting activity of REF-1 in K-1034 cells was dose dependent, with a bell-shaped curve (Fig. 5a), perhaps because of the downregulation of receptor at a higher REF-1 concentration.

The growth-promoting activities of other relevant cytokines, TFPI-1, CNTF, and bFGF on RPE cells were compared at a 10-ng/mL concentration. TFPI-1 is a member of the TFPI family with 35% amino acid sequence homology with TFPI-2; however, RPE cells did not respond to TFPI-1. CNTF, a human ciliary nerve nutritional factor, also did not stimulate RPE cell proliferation. However, the growth stimulation of bFGF was stronger than that of REF-1 (Fig. 5b).

Growth stimulation of HUVECs, human fibroblasts, rabbit primary RPE cells, and fourth-passage human primary RPE cells was also examined (Fig. 5c). A 12% and 25% increase after

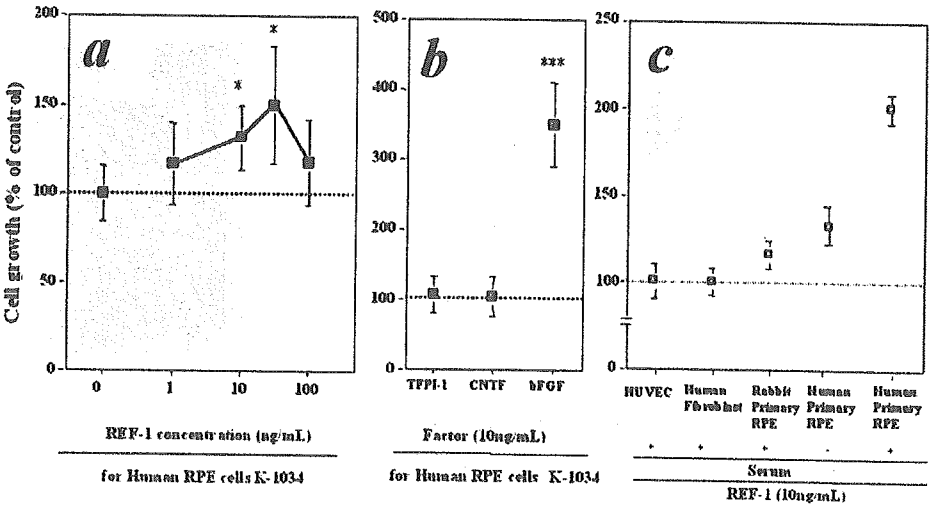

FIGURE 5. Cell proliferation activity of recombinant REF-1. Dose-dependent REF-1 activity in human K-1034 RPE cells (**a**), growth-promoting activities of TFPI-1, CNTF, and bFGF in human K-1034 RPE cells (**b**), and proliferative response of HUVECs, human fibroblast, rabbit primary RPE cells, and human primary RPE cells to 10 ng/mL REF-1 (**c**).

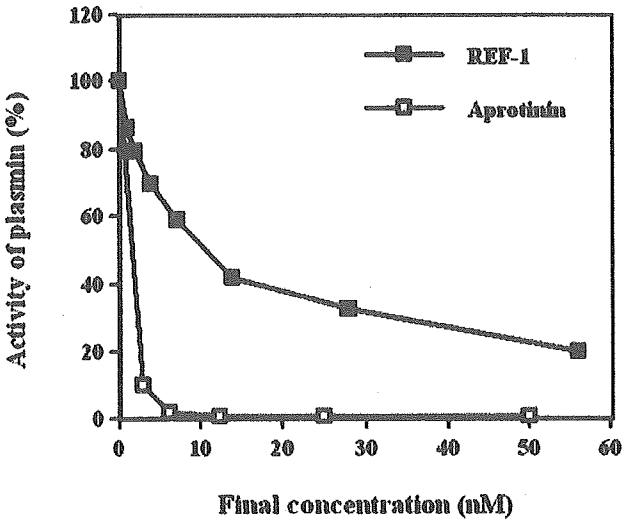

FIGURE 6. Protease inhibitory activity of REF-1. The residual activities of plasmin with aprotinin (positive control, 4 μg/mL) or REF-1/TFPI-2 (5 μg/mL) were determined, in 96-well plastic plates, with S-2251 (Val-Leu-Lys-pNA, 1 mg/mL) used as a substrate. The percentage of relative activity in the inhibitor concentration was calculated from absorbance at 405 to 450 nm.

stimulation by REF-1 was observed in rabbit primary RPE cells and human primary RPE cells, respectively. Significant proliferation was observed in human primary RPE cells cultured in medium with 15% FCS.

Proteinase Inhibitory Activity

REF-1 inhibited plasmin (Fig. 6), and it was confirmed that it inhibited serine protease.

Determination of REF-1 in Human Primary RPE Cells

The existence of REF-1 was determined in human primary RPE cells by Western blot analysis and RT-PCR (Fig. 7). REF-1 was not detected in RPE cells by Western blot under the conditions we used; however, REF-1 mRNA was detected in total RNA extracted from human primary RPE cells by 30 cycles of PCR.

Effect of REF-1 Treatment on Cytokine Production of RPE Cells

Eleven cytokines and growth factors were measured in serum-free culture medium of fourth-passage human primary RPE cells treated with 10 ng/mL of REF-1 for 2 days. TGF-β1 and GM-CSF were significantly induced by 4.7- and 2.4-fold, respectively. bFGF, IL-6, IL-8, and M-CSF showed no or only a moderate increase with REF-1 treatment. TGF-β2, IL-1β, G-CSF, TNF-α, and EGF were undetectable (Table 2).

DISCUSSION

We have isolated and identified a biologically active protein that stimulated RPE cell to proliferate and consider it to be a potential therapeutic agent. This factor has growth-promoting properties that it exerts on RPE cells and was identified as REF-1 protein. Molecular cloning showed that this factor was homologous to the TFPI-2/PP5 protein. The RPE cell growth-promoting effect of REF-1/TFPI-2 was found to be more specific to RPE cells than to fibroblasts and HUVECs. Currently, there are no reports of factors that specifically stimulate the growth of RPE cells, although several growth factors such as bFGF, EGF, PDGF, and VEGF are growth promoters. These factors also have other properties, such as angiogenesis and potential stimulation of endothelial cell growth and can cause proliferative vitreoretinopathy by fibroblast proliferation. These undesirable properties do not allow them to be used for the treatment of retinal diseases. Although REF-1/TFPI-2 has a relatively weaker growth-promoting action than bFGF in vitro, it did not stimulate endothelial cell growth or fibroblast proliferation. Thus, the specificity of REF-1/TFPI-2 to RPE cells is greater than that of other growth factors (Fig. 5).

We determined the growth-promoting activity of REF-1/TFPI-2 using 10th- to 20th-passage human K-1034 RPE cells, primary HUVECs, primary rabbit RPE cells, and 4th-passage primary human RPE cells. Early-passage RPE cells responded

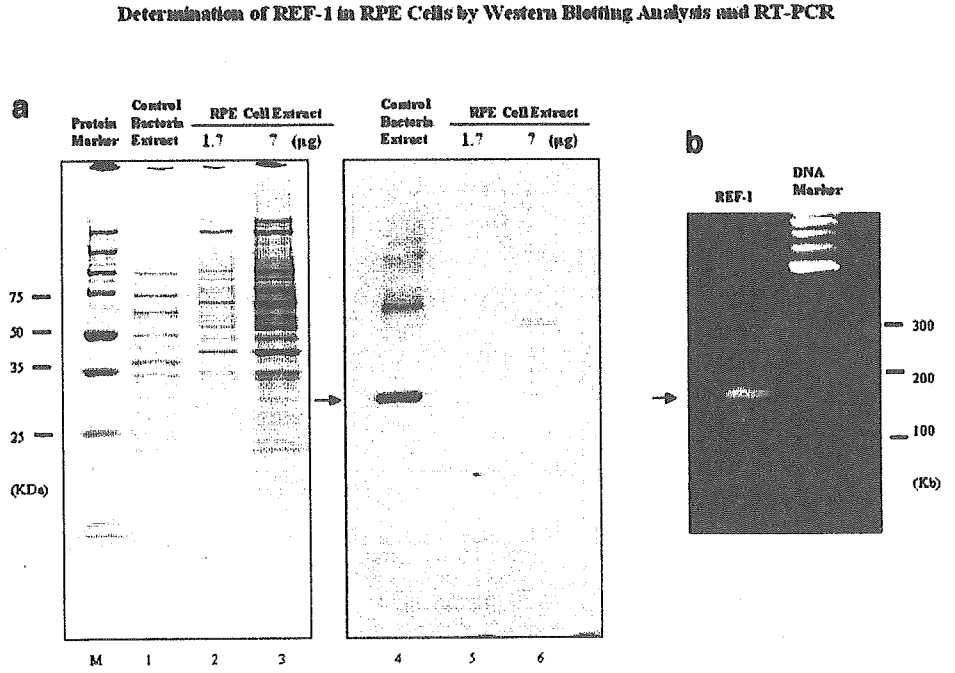

FIGURE 7. Determination of REF-1 in human primary RPE cells. REF-1 in human primary RPE cells was determined by Western blot analysis or RT-PCR. (a) Western blot of REF-1 for human primary RPE cell extract. *Lane 1*: Coomassie staining of bacteria extract expressing recombinant REF-1 (34 kDa); *lane 2*: Coomassie staining of human RPE cell extract (1.7 μg); *lane 3*: Coomassie staining of RPE cell extract (7 μg); *lane 4*: Western blot of bacteria extract expressing recombinant REF-1 (34 kDa); *lane 5*: Western blot of RPE cell extract (1.7 μg); *lane 6*: Western blot of RPE cell extract (7 μg). (b) RT-PCR of REF-1 transcript in total RNA extracted from human primary RPE cells. A single band was observed after 30 cycles of amplification.

TABLE 2. Production of Cytokines by Human Primary RPE Cells Treated with REF-1 (10 ng/mL)

Cytokine	REF-1 (pg/10^5 cells)		
	−	+	+/−
bFGF	508	546	1.0
TGF-β1	673	3163	4.7
TGF-β2	Nondetectable	Nondetectable	—
IL-1β	Nondetectable	Nondetectable	—
IL-6	1770	1922	1.1
IL-8	556	837	1.5
G-CSF	Nondetectable	Nondetectable	—
GM-CSF	817	1959	2.4
M-CSF	420	509	1.2
TNF-α	Nondetectable	Nondetectable	—
EGF	Nondetectable	Nondetectable	—

satisfactorily to REF-1; however, aged K-1034 RPE cells did not (data not shown), whereas primary rabbit RPE cells and primary HUVECs responded poorly to REF-1. Aged K-1034 RPE cells retained their response to basic FGF as well as early-passaged cells. These observations indicate that the growth-promoting effect of RPE-1 may be age-related and that it probably stimulates growth by a pathway different from that used by other growth factors such as bFGF. Although, growth stimulation was observed for human primary RPE cells in both serum-free and serum-added medium, REF-1 favored the latter condition, resulting in fourfold proliferation. Exogenous factor(s) may be involved in this effect.

Our experiments showed that at least 2 of 11 cytokines were stimulated by REF-1 treatment. To our surprise, TGF-β1 production was significantly induced (4.7-fold) in REF-1-treated compared with nontreated cells. A possible explanation for this phenomenon is that TGF-β1 production is stimulated to suppress and balance the rapid growth rate of RPE cells. This suggestion may be supported by the inhibitory effect of TGF-β1 on RPE cell proliferation.[21]

Another cytokine, increased by 2.4-fold, was colony-stimulating factor GM-CSF. GM-CSF is known to be an important regulator of macrophage, granulocyte, dendritic cell, and eosinophil behavior.[22,23] RPE cells have properties similar to macrophages—that is, to phagocytose and generate different cytokines, including GM-CSF.[24] In RPE cells, GM-CSF has been reported to be upregulated in response to TNF-α,[24] IL-1α,[25] or IL-1β[26] and downregulated by IFN-γ.[26] The signal transduction mechanism for upregulation of GM-CSF by REF-1 is currently under investigation.

REF-1 was detected by RT-PCR in human primary RPE cells after 30 cycles of PCR; however, Western blot analysis failed to detect REF-1 in the experimental conditions we used. REF-1 mRNA may require specific stimulation to produce protein in RPE cells.

TFPI-2 has been shown to act as an anticoagulant[8] and serine protease inhibitor.[9] It is unclear whether these activities are correlated with growth promotion. Recent studies on TFPI-2 have shown that it has novel biological effects, such as inhibition of matrix metalloproteinase (MMP),[15,16] promotion of smooth muscle growth,[17] and modulation of melanoma and glioma invasion.[18,19] The relationship between these activities and promotion of RPE cell proliferation is still unknown. TFPI-2/REF-1 has been found in human ciliary epithelium[20] and may play an important role in the normal RPE environment. It also has potential for therapeutic use for ocular tissue damage. To confirm these possibilities further pharmacological evaluations in vivo are needed, using suitable animal models and effective drug delivery methods to the damaged sites.

References

1. Marmor MF. Introduction to structure, function, and diseases of the retinal pigment epithelium. In: Marmor MF, Wolfensberger TJ. *The Retinal Pigment Epithelium: Function and Disease*. London, UK: Oxford University Press. 1998;3–12.
2. Hackett SF, Schoenfeld CL, Freund J, Gottsch JD, Bhargave S, Campochiaro PA. Neurotrophic factors, cytokines and stress increase expression of basic fibroblast growth factor in retinal pigmented epithelial cells. *Exp Eye Res*. 1997;64:865–873.
3. Campochiaro PA, Glaser BM. Platelet-derived growth factor is chemotactic for human retinal pigment epithelial cells. *Arch Ophthalmol*. 1985;103:576–579.
4. Kaven CW, Spraul CW, Zavazava NK, Lang GK, Lang GE. Growth factor combinations modulate human retinal pigment epithelial cell proliferation. *Curr Eye Res*. 2000;20:480–487.
5. Schweigerer L, Neufeld G, Friedman J, Abraham JA, Fiddes JC, Gospodarowicz D. Capillary endothelial cells express basic fibroblast growth factor, a mitogen that promotes their own growth. *Nature*. 1987;325:257–259.
6. Cassidy L, Barry P, Shaw C, Duffy J, Kennedy S. Platelet derived growth factor and fibroblast growth factor basic levels in the vitreous of patients with vitreoretinal disorders. *Br J Ophthalmol*. 1998;82:181–185.
7. Kliffen M, Sharma HS, Mooy CM, Kerkvliet S, de Jong PT. Increased expression of angiogenic growth factors in age-related maculopathy. *Br J Ophthalmol*. 1997;81:154–162.
8. Sprecher CA, Kisiel W, Mathewes S, Foster DC. Molecular cloning, expression, and partial characterization of a second human tissue-factor-pathway inhibitor. *Proc Natl Acad USA*. 1994;91:3353–3357.
9. Miyagi Y, Koshikawa N, Yasumitsu H, et al. cDNA cloning and mRNA expression of a serine proteinase inhibitor secreted by cancer cells: identification as placental protein 5 and tissue factor pathway inhibitor-2. *J Biochem*. 1994; 116:939–942.
10. Utsumi J, Iizuka M, Kobayashi S. Interferon production with multitray culture system on a large scale. *J Interferon Res*. 1984;4:9–16.
11. Kigasawa K, Soushi S, Tanaka Y, Obazawa H. Morphologic and chromosomal study of a human retinal pigment epithelial cell line. *Jpn J Ophthalmol*. 1994;38:10–15.
12. Sano E, Okano K, Sawada R, et al. Constitutive long-term production and characterization of recombinant human interferon-gammas from two different mammalian cells. *Cell Struct Funct*. 1988; 13:143–159.
13. Petersen LC, Sprecher CA, Foster DC, Blumberg H, Hamamoto T, Kisiel W. Inhibitory properties of a novel human Kunitz-type protease inhibitor homologous to tissue factor pathway inhibitor, *Biochemistry*. 1996;35:266–272.
14. Rao CN, Reddy P, Liu Y, et al. Extracellular matrix-associated serine protease inhibitors (Mr. 33, 000, 31.000, and 27, 000) are single-gene products with differential glycosylation: cDNA cloning of the 33-kDa inhibitor reveals its identity to tissue factor pathway inhibitor-2. *Arch Biochem Biophys*. 1996;335:82–92.
15. Rao CN, Mohanam S, Puppala A, Rao JS. Regulation of proMMP-1 and ProMMP-3 activation by tissue factor pathway inhibitor-2/matrix-associated serine protease inhibitor. *Biochem Biophys Res Commun*. 1999;255:94–98.
16. Herman MP, Sukhova GK, Kiesiel W, et al. Tissue factor pathway inhibitor-2 is a novel inhibitor of matrix metalloproteinases with implication for atherosclerosis. *J Clin Invest*. 2000;107:1117–1126.
17. Shinoda E, Yui Y, Hattori R, et al. Tissue factor pathway inhibitor-2 is a novel mitogen for vascular smooth muscle cells. *J Biol Chem*. 1999;274:5379–5384.
18. Konduri SD, Tasiou A, Chandrasekar N, Nicolson GL, Rao JS. Role of tissue factor pathway inhibitor-2 (TFPI-2) in amelanotic melanoma (C-32) invasion. *Clin Exp Metastasis*. 2000;18:303–308.
19. Konuri SD, Rao CN, Chandrasekar N, et al. A novel function of tissue factor pathway inhibitor-2 (TFPI-2) in human glioma invasion. *Oncogene*. 2001;20:6938–6945.

20. Ortego J, Escribano J, Coca-Prados M. Gene expression of proteases and protease inhibitors in the human ciliary epithelium and ODM-2 cells. *Exp Eye Res.* 1997;65:289–299.
21. Lee SC, Seong GJ, Kim SH, Kwon OW. Synthesized TGF-beta s in RPE regulates cellular proliferation. *Kor J Ophthalmol.* 1999;13:16–24.
22. Gasson JC, Molecular physiology of granulocyte-macrophages colony stimulating factors. *Blood.* 1991;77:1131–1145.
23. Fischer HG, Frosch S, Reske K, Reske-Kunz AB. Granulocyte-macrophages colony-stimulating factor activates macrophages derived from bone marrow cultures to synthesis of MHC class II molecules and to augmented antigen presentation. *J Immunol.* 1988;141:3882–3888.
24. Crane IJ, Kuppner MC, McKillop-Smith S, Wallace CA, Forrester JV. Cytokine regulation of granulocyte-macrophage colony-stimulating factor (GM-CSF) production by human retinal pigment epithelial cells. *Clin Exp Immunol.* 1999;115:288–293.
25. Plank SR, Huang X-N, Robertson JE, Rosenbaum JT. Retinal pigment epithelial cells produce interleukin-1β and granulocyte-macrophage colony-stimulating factor in response to interleukin-1α. *Curr Eye Res.* 1993;12:205–212.
26. Crane IJ, Wallace CA, Forrester JV. Regulation of granulocyte-macrophage colony-stimulating factor in human retinal pigment epithelial cells by IL-1β and IFN-γ. *Cell Immunol.* 2001;209:132–139.

Analysis of Porcine Optineurin and Myocilin Expression in Trabecular Meshwork Cells and Astrocytes from Optic Nerve Head

Minoru Obazawa,[1,2] *Yukihiko Mashima,*[2] *Naoko Sanuki,*[1] *Setsuko Noda,*[3] *Jun Kudoh,*[4] *Nobuyoshi Shimizu,*[4] *Yoshihisa Oguchi,*[2] *Yasuhiko Tanaka,*[1] *and Takeshi Iwata*[1]

Purpose. To determine the cDNA sequences and analyze the expression of porcine optineurin and myocilin in trabecular meshwork cells (TMCs) and astrocytes from the optic nerve head under normal and experimental conditions.

Methods. Both porcine optineurin and myocilin were cloned to determine the cDNA sequences. Porcine TMCs and astrocytes were isolated and treated with dexamethasone (500 nM) for 2 weeks, incubated under hypoxic conditions (7% O_2) for 72 hours, or exposed to 33 mm Hg hydrostatic pressure for 72 hours. A 10% mechanical stretch for 24 hours was also performed on TMCs. The expression level of the optineurin and myocilin transcripts was analyzed by real-time quantitative PCR.

Results. The sequences of porcine optineurin and myocilin cDNA were determined, and the expression of both genes was confirmed in both TMCs and astrocytes. Amino acid sequences of porcine optineurin and myocilin were homologous to those of humans by 84% and 82%, respectively, and shared protein motifs and modification sites. The expression of myocilin mRNA by TMCs and astrocytes was increased by 8.0- and 5.5-fold, respectively, after exposure to dexamethasone. In contrast, the expression of optineurin was suppressed to 68% in TMCs and 48% in astrocytes after exposure to dexamethasone. A significant reduction of myocilin expression was observed after 72 hours of incubation under hypoxic conditions in both types of cells, whereas optineurin was not affected. Hydrostatic pressure for 72 hours and mechanical stretching for 24 hours had minimal affects on gene expression of both optineurin and myocilin.

Conclusions. The high homology of porcine optineurin and myocilin to the comparable human genes indicates that pigs can be used to study changes in gene expression in hypertensive eyes. The alterations in expression of myocilin but not of optineurin under stress suggest that different mechanisms in the phenotype of glaucoma associated with the two genes are involved in development of glaucoma. (*Invest Ophthalmol Vis Sci.* 2004;45:2652–2659) DOI:10.1167/iovs.03-0572

Characteristic degeneration and excavation of the optic nerve head are found in glaucomatous eyes. These changes are considered to be due to ocular hypertension with the intraocular pressure (IOP) continuously more than 21 mm Hg. In contrast, there are patients with normal ocular tension who show glaucomatous changes in the optic nerve head. These patients, in whom there is no evidence of an elevation of IOP at any time, are said to have normal-tension glaucoma (NTG).

Currently three genes—myocilin (*MYOC*),[1,2] cytochrome P4501B1 (*CYP1B1*),[3,4] and optineurin (*OPTN*)[5]—are associated with glaucoma. Optineurin is the most recent gene to be identified and is responsible for 16.7% of families with hereditary NTG.[5] It has been identified and studied by different groups under various names: NRP, NF-κB essential modulator (NEMO)-related protein[6]; FIP-2, adenovirus E3-14-kDa interacting protein 2[7]; Huntingtin interacting protein L (HYPL)[8]; and transcription factor IIIA interacting protein (TFIIIA-INTP).[9] Optineurin is homologous to NEMO, a structural and regulatory subunit of the high molecular weight kinase complex (IKK) that is responsible for the phosphorylation of NF-κB inhibitors.[6]

Some of the functions of optineurin are known. They include inhibition of the tumor necrosis factor (TNF)-α pathway,[7] interaction with transcription factor IIIA,[9] and mediation of the interaction of Huntingtin and Rab8 for regulation of membrane trafficking and cellular morphogenesis.[8] Optineurin is induced by TNF-α and binds to an inhibitor of TNF-α and the E3-14.7-kDa protein.[7]

The optineurin protein contains two leucine zippers (LZs); an N-terminal LZ responsible for the association with Rab8, and a C-terminal LZ required for Huntingtin. The gene is mapped to 10p14 and contains 16 exons encoding a 66-kDa protein. It contains two putative bZIP transcription factor motifs, a C2H2 type zinc finger, and two LZ domains.

Recently, Vittitow and Borrás[10] reported that elevated IOP, and exposure to TNF-α and dexamethasone (DEX) led to an upregulation of optineurin expression in an organ culture system. However, it is still unclear how mutations of the optineurin gene lead to glaucoma.

Another gene associated with glaucoma is myocilin, which is found in 36% of juvenile-onset POAG and 4% of adult-onset POAG.[11–15] Myocilin is a 57-kDa protein that contains motifs homologous to the olfactomedin domain where nearly all mutations in patients with POAG have been identified.[1,11–15]

Pigs and miniature pigs are readily available and have been used for a wide variety of medical studies, including tissue transplantation.[16,17] Because their eyes are similar in size and

From the [1]National Institute of Sensory Organs, National Tokyo Medical Center, Tokyo, Japan; the Departments of [2]Ophthalmology and [4]Molecular Biology, Keio University School of Medicine, Tokyo, Japan; and the [3]Department of Nursing, School of Health Science, Tokai University, Isehara, Kanagawa, Japan.

Supported by Research on Eye and Ear Sciences from the Ministry of Health, Labor, and Welfare, Japan; a grant for Scientific Research and Exploratory Research from the Ministry of Education, Science, Sports, and Culture of Japan; and funding from the Research for the Future Program from the Japan Society for the Promotion of Science.

Submitted for publication June 7, 2003; revised December 1, 2003; accepted December 8, 2003.

Disclosure: **M. Obazawa**, None; **Y. Mashima**, None; **N. Sanuki**, None; **S. Noda**, None; **J. Kudoh**, None; **N. Shimizu**, None; **Y. Oguchi**, None; **Y. Tanaka**, None; **T. Iwata**, None

The publication costs of this article were defrayed in part by page charge payment. This article must therefore be marked "*advertisement*" in accordance with 18 U.S.C. §1734 solely to indicate this fact.

Corresponding author: Takeshi Iwata, Laboratory of Cellular and Molecular Biology, National Institute of Sensory Organs, National Tokyo Medical Center, 2-5-1, Higashigaoka, Meguro, Tokyo 152-8902, Japan; iwatatakeshi@kankakuki.go.jp.

Investigative Ophthalmology & Visual Science, August 2004, Vol. 45, No. 8

anatomy to human eyes,[18] pigs have often been used to study the aqueous outflow system and the regulation of IOP.

The purpose of this study was to clone both the porcine optineurin and myocilin genes to determine their cDNA sequences, and then to use the sequences to determine the transcriptional response of isolated porcine trabecular meshwork cells (TMCs) and astrocytes from the optic nerve head after exposure to dexamethasone (DEX), increased hydrostatic pressure, hypoxia, and mechanical stretching.

Materials and Methods

Cell Cultures

Pig eyes were obtained within 3 hours of death from a local abattoir. The eyes were disinfected in 0.2% povidone iodine for 10 minutes followed by soaking in 70% alcohol for 30 seconds. The eyes were washed several times in phosphate-buffered saline (PBS) and cut into halves along the equator.

After the lens and iris were removed from the anterior half, the trabecular tissue was trimmed from the cornea at the Schwalbe's line and then from the sclera, as described.[19,20] The optic nerve head was separated from the sclera and surrounding tissues. The prelaminar region was dissected from the optic nerve head and cut into three or four pieces.[21,22] The trabecular and prelaminar tissues were placed separately in 35-mm plastic Petri dishes in Dulbecco's modified Eagle's medium (DMEM; Invitrogen-Gibco, Grand Island, NY) with 10% fetal bovine serum (Sigma-Aldrich, St. Louis, MO) and 1% antibiotic-antimycotic (Invitrogen-Gibco).

The tissues were incubated for 1 to 2 weeks at 37°C in humidified 5% CO_2 and 95% air until cells migrated from the tissue onto the surface of the culture dish. Cells were isolated, and fourth-passage cells were obtained for experimental use. The cells that migrated from the optic nerve head were confirmed to be astrocytes by immunostaining with anti-glial fibrillary acidic protein (GFAP), a protein marker for astrocytes (Sigma-Aldrich).

Cloning of Porcine Optineurin cDNA

mRNA was isolated from cultured TMCs using mRNA isolation kits (MicroPoly(A)Pure; Ambion, St. Austin, TX). Primers (sense primer, 5′-ATGTCCCATCAACCTCTGAGCT-3′, antisense primer 5′-TGTCCTCGGCTCCTCTTTGAAA-3′) were designed to include the conserved sequences for human, mouse (Discovery System; Celera, Gaithersburg, MD), and rat to amplify the open reading frame of porcine optineurin mRNA using a commercial system (Superscript One-Step RT-PCR System; Invitrogen-Gibco), according to the manufacturer's protocol.

The PCR products were cloned into a TA cloning vector (pDrive; Qiagen, Valencia, CA) using a PCR Cloning Kit (Qiagen), and the inserts were sequenced using a fluorescent dideoxynucleotide automated sequencer (CEQ2000XL DNA Analysis System; Beckman-Coulter, Fullerton, CA). The missing 3′ and 5′ ends of the cDNAs were amplified using the 3′ and 5′ rapid amplification of cDNA ends (RACE) method (Marathon cDNA Amplification Kit; BD Biosciences-Clontech, Palo Alto, CA). The full-length cDNA sequence of porcine optineurin can be obtained from GenBank under accession number AF513722 (http://www.ncbi.nlm.nih.gov/Genbank; provided in the public domain by the National Center for Biotechnology Information, Bethesda, MD).

Cloning of Porcine Myocilin cDNA

The same mRNA used for optineurin cDNA cloning was used for myocilin cDNA amplification. The sense primer, 5′-ATGCCAGCTS(G/C)TCCAGCTGCT-3′, and antisense primer, 5′-GACCATGTTGAAGTTGTCCCA-3′, were designed to include the conserved sequence of human, mouse, rat, and bovine myocilin and to amplify the open reading frame of porcine myocilin mRNA, using the RT-PCR system (Superscript One-Step RT-PCR System; Invitrogen-Gibco). The PCR products were cloned into a TA cloning vector (TA Cloning Kit; Invitrogen, San Diego, CA), and the inserts were sequenced. The missing 3′ and 5′ ends of the cDNA were amplified using the RACE method (Marathon cDNA Amplification Kit; BD Biosciences-Clontech). The full-length cDNA sequence of porcine myocilin can be obtained from GenBank under accession number AF350447.

Sequence Analysis of Porcine Optineurin and Myocilin

Amino acid sequences of both optineurin and myocilin were analyzed for domain structure and potential protein modification sites. The PROSITE scanning tool[23] (http://www.nhri.org.tw/prosite/; provided in the public domain by the Swiss Institute of Bioinformatics, Geneva, Switzerland) was used to scan the optineurin protein sequence for the occurrence of patterns and profiles stored in the PROSITE database. Potential glycosylation and phosphorylation sites were predicted by the program developed by Hansen et al.,[24] and Blom et al.,[25] respectively. Sequence homology was determined by a sequence-analysis program (Omiga 2.0; Accelrys, San Diego, CA).

Stress Experiments for Optineurin and Myocilin

All stress experiments were performed using fourth-passage TMCs and astrocytes from three different porcine eyes. For the DEX treatment, DEX stock solution (50 mM DEX/dimethyl sulfoxide) was added to cultured TMCs and astrocytes at a final concentration of 500 nM. The culture medium was replaced every 3 days and maintained for 2 weeks. For control, cultured cells were treated with dimethyl sulfoxide alone.

To examine the effect of hypoxia, both types of cultured cells were incubated in 7.0% O_2 and 5% CO_2, in a multiple gas incubator (model 9200; Wakenyaku, Kyoto, Japan) for 12, 24, 48, or 72 hours. Control cells were incubated for the same times in 5% CO_2 and 95% air in a standard CO_2 incubator.

To examine the effects of hydrostatic pressure, we exposed both types of cultured cells to a hydrostatic pressure of 33 mm Hg above atmospheric pressure for 12, 24, 48, or 72 hours in a CO_2 incubator, using the system illustrated in Figure 1. The culture flasks were filled with the medium and capped with a silicon stopper to prevent leakage. The height of the reservoir containing the medium was adjusted to control the pressure in the flask. For gas exchange, the medium was circulated with a peristaltic pump (Eyela, Tokyo, Japan), and the pressure was monitored with a pressure gauge (model PG-208; Copal Electronics, Tokyo, Japan). Control cells were exposed to hydrostatic pressure of 3 mm Hg above atmospheric pressure for 12, 24, 48, and 72 hours.

To examine the effects of mechanical stretching, cultured porcine TMCs were transferred onto a 10-cm^2 collagen-coated silicon chamber (S.Tec, Osaka, Japan). The silicon chamber had a 100-μm-thick transparent bottom, and the side walls were 1.5-mm thick to prevent narrowing at the bottom center. The silicon chamber was then attached to a stretching apparatus for a 10% linear stretch for 24 hours in a standard CO_2 incubator. Control cells were plated onto a collagen-coated silicon chamber without the stretching for the same amount of time.

Optineurin and Myocilin Transcript Analysis

Total RNA was isolated from cultured cells exposed to stimuli or stresses (RNAzol B; Tel-Test, Friendswood, TX). The total RNA was reverse transcribed (Superscript First Strand Synthesis System for RT-PCR; Invitrogen-Gibco) according to the manufacturer's protocol. Real-time quantitative PCR was performed to determine the optineurin, myocilin, and glyceraldehyde-3-phosphate dehydrogenase (GAPDH) transcript with a sequence-detection system (GeneAmp 5700; Applied Biosystems, Inc. [ABI], Foster City, CA). PCR reactions were performed in 50 μL of reaction mixture containing 25 μL master PCR mix (SYBR Green PCR Master Mix; ABI), 5 pM primer pairs, and 1 μL cDNA samples. To measure myocilin transcript, 4 μL cDNA samples was used because of lower expression. The 18S ribosomal RNA gene was used as